Russian Chemical Reviews **75** (1) 1 – 22 (2006) © 2006 Russian Academy of Sciences and Turpion Ltd

DOI 10.1070/RC2006v075n01ABEH001203

New horizons of chemistry: single molecules

A L Buchachenko

Contents

I.	Single molecules as investigation subjects	1
II.	Luminescence of single molecules	1
III.	Scanning tunnelling spectroscopy	7
IV.	A single high-spin molecule as a nanomagnet	12
V.	Raman spectroscopy of single molecules	14
VI.	Electrical conductivity of single molecules	15
VII.	Mechanics and mechanochemistry of single molecules	17
VIII.	Conclusion	20

Abstract. The chemistry has reached its upper boundary, *i.e.*, the ability to detect, fix in space and identify a single molecule, measure almost any of its properties and observe its chemical transformations and functioning. At this frontier, procedures for manipulating single molecules are developed and the element base for nanooptics, nanomechanics and nanoelectronics is created. This is the prologue for a new technological civilisation, *viz.*, to molecular electronics which operates with electric voltages of the order of millivolts and electric currents of the order of nanoamperes. The bibliography includes 101 references.

I. Single molecules as investigation subjects

At the boundary of the 20 and 21 centuries, a quiet revolution almost unnoticed by the broad scientific community took place in chemistry and molecular physics, namely, a breakthrough in the experimental techniques for detection and identification of single molecules and manipulation of them. Luminescence, electrical conductivity, magnetism, non-linear optics, electron paramagnetic and nuclear magnetic resonances, atomic vibration frequencies, elasticity and strength, *i.e.*, all the parameters and properties that have been measured previously only for large ensembles of molecules are now measured also for a single molecule.

This review gives analysis of the key ideas and concepts in the chemistry, physics and mechanics of single molecules. Their significance for chemistry is formulated.

First, detection of a single molecule corresponds to the limit of detection in analytical chemistry. For 'readout' of one molecule on a 1 μm^2 surface from a 1 μm-thick layer (nowadays, this is the normal 'operating' condition), the concentration detection limit is 10^{15} litre^{-1} or 10^{-9} mol litre^{-1}. This boundary is meant in the design of detectors of single molecules and highest-sensitivity sensors.

Second, it becomes possible to establish the individual, 'personal' properties of a single molecule rather than averaged or 'hidden' in a large ensemble of similar molecules. Any spectroscopy of large ensembles exhibits non-uniform broadening of spectral lines, which are superpositions of a multitude of lines (differing in widths and frequencies) from the multitude of molecules occurring in different environments. 'Extracting' the spectrum of an individual molecule from the superposition of lines is a complicated and ambiguous task. The spectroscopy of single molecules normally does not face this problem. The spectrum of a single molecule is a reliable and sensitive test of its local environment (molecular site), *i.e.*, the place occupied by the molecule and its near surrounding.

Third, it is now possible to observe functioning of a single molecule and answer the question of how it works, either continuously or with 'rest' periods, in a time-correlated mode or its functioning is random, whether or not it retains the 'memory' of the preceding events of its 'life.' Actually, this is a new field of molecular knowledge which we are only starting to enter.

Fourth, while developing the techniques for manipulation of single molecules (their migration, joining, insertion and combination to form specified molecular ensembles), researchers acquire the experience in designing elements of nanoelectronics, nanomechanics, nanooptics — the future high technology. This is not just a declaration; this is real work on the route of research and discoveries.[1]

II. Luminescence of single molecules

The principle of optical detection of single molecules is simple: laser irradiation of a surface containing luminescent molecules excites their luminescence and they can be detected as molecular 'glow-worms'. In Fig. 1 *a* one can see signals from 'luminous' rhodamine B molecules dispersed on the surface of a poly(methyl methacrylate) film;[2] the site from which the radiation is collected is 4.5×4.5 μm. Figure 1 *b* shows the signals from single molecules of the enzyme cholesterol oxidase embedded into an agarose gel film.[3] Flavin adenine dinucleotide is the emitter in the enzyme molecule. Light is collected from a 8×8 μm area which accommodates only several molecules. The flickering glow of one cholesterol oxidase molecule is shown in Fig. 1 *c*.[3]

Since the first observations of the luminescence of single molecules (the late 1980s),[4] the techniques and technology of optical detection have substantially progressed as regards both sensitivity and reliability.[5, 6] Scanning optical microscopes, high-sensitivity photoelectric detectors, and near-field microscopy

A L Buchachenko Institute of Problems of Chemical Physics, Russian Academy of Sciences, 142432 Chernogolovka, Moscow Region, Russian Federation. Fax (7-496) 524 96 76, tel. (7-495) 939 71 28, e-mail: spinchem@chph.ras.ru, abuchach@chph.ras.ru

Received 25 March 2005
Uspekhi Khimii **75** (1) 3 – 26 (2006); translated by Z P Bobkova

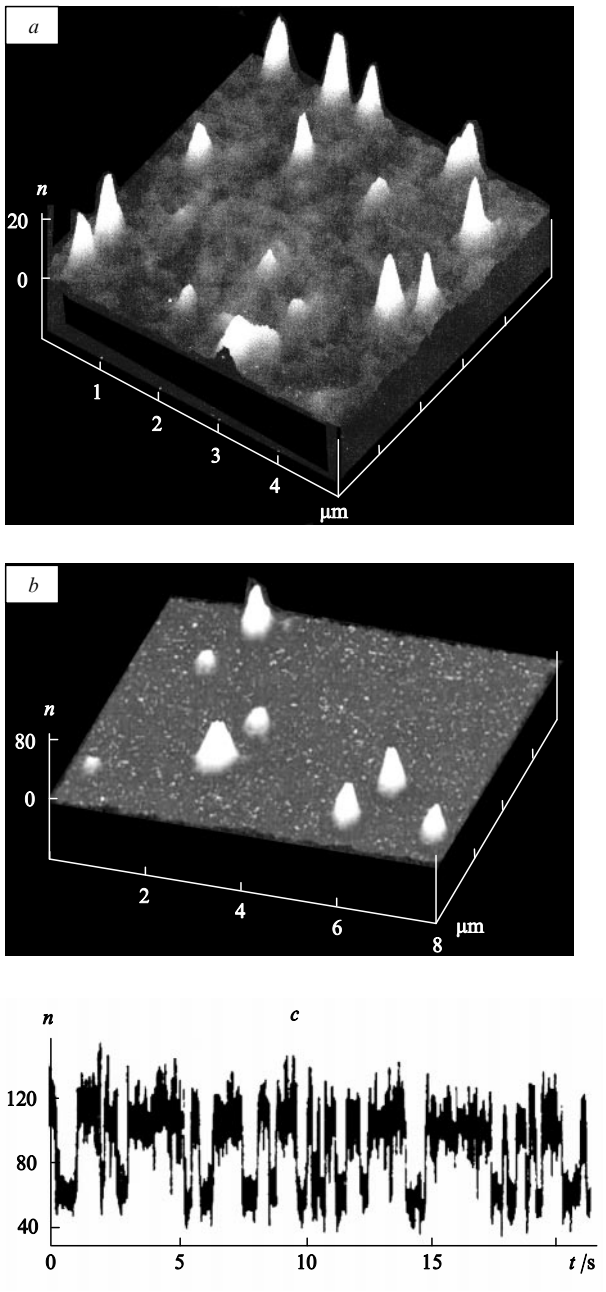


Figure 1. Image of the luminescence of single molecules: (*a*) rhodamine B on poly(methyl methacrylate) (the drawing was taken from Ref. 2); (*b*) cholesterol oxidase in the agarose gel (the drawing was taken from Ref. 3); (*c*) 'flickering' of one cholesterol oxidase molecule with time (*n* is the number of photons emitted per unit time).

opened up the access to detection of luminescent molecules and luminescent labels in solids and liquids, on surfaces and at interfaces, in monolayers and Langmuir – Blodgett films, in liquid crystals and gels, emulsions and porous media, membranes, proteins, nucleic acids, enzymes, chromosomes and molecular motors.[7,8] A procedure has been developed for detecting luminescent molecules in microcapillaries and microdrops (hanging or dropping), during electrophoresis and in the tunnelling microscope cavity in which luminescence is excited by the tunnelling current.[9] The range of luminophores (emitters having a high photostability and a great quantum yield) used for attachment to biomacromolecules as luminescent labels and suitable for being placed into any medium has been markedly extended.[7]

A two-quantum luminescence excitation process has been developed. In this case, a molecule is excited by a long-wavelength radiation, the emission being detected in the short-wave region; this sharply decreases the scattered optical background in the luminescence band and increases the signal-to-noise ratio and, hence, the sensitivity.

Now we consider what new information useful for chemistry is provided by the optical detection of single molecules.

1. Testing of molecular sites

From classical luminescence measurements, one can derive information on averaged properties and interactions of a large ensemble of molecules (even when these are identical). The spectroscopy of a single molecule rules out the averaging. The data obtained by detecting a set of single molecules are much more valuable. The frequency, intensity, line width and polarisation of the luminescence of a single molecule depend on its local environment (local compression, crystal density, vacancies, the presence of quenchers) and on its interaction with the environment (through acoustic phonons and local vibrations). Actually, a single molecule is a 'reporter' providing information on the molecular site occupied by the molecule and on the events taking place in this site. An example of this 'running commentary' is shown in Fig. 2.[10] Figure 2 *a* shows a series of the fluorescence spectra of pentacene in a *p*-terphenyl crystal at 1.5 K; each spectrum was recorded for 2.5 s (at 0.25 s intervals). It can be seen that the radiation frequency of pentacene varies randomly and unpredictably (every time fluorescence is excited at a different laser frequency; the variation of this frequency is laid-off along the abscissa axis). This means that the energy state of the reporter molecule also varies randomly. The wandering of the molecule over its energy

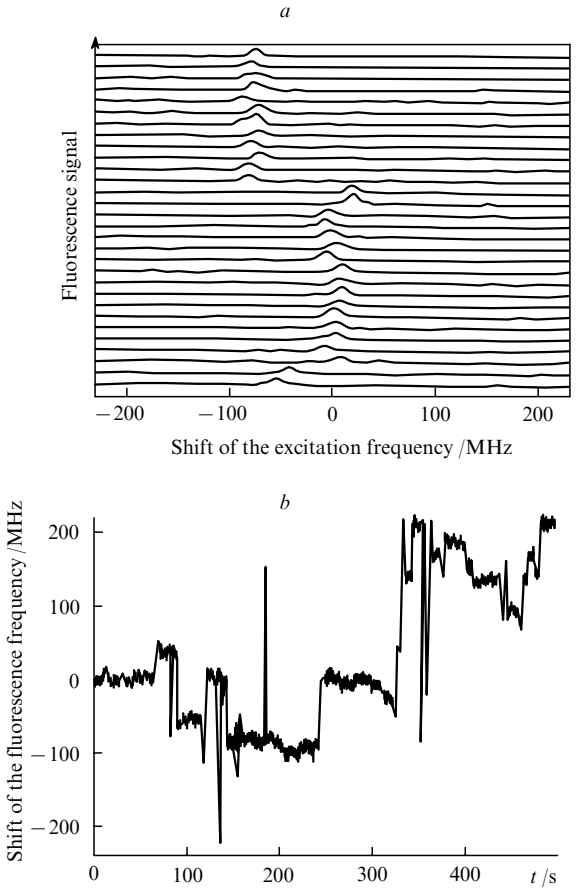


Figure 2. Spectral diffusion of pentacene in *p*-terphenyl at 1.5 K. (*a*) successive fluorescence records showing random shifts of the excitation frequency (recording duration 2.5 s, spacing between the records 0.25 s); (*b*) path of the variation of the fluorescence frequency during the detection of the spectra (500 s).[10]

states (*i.e.*, over the luminescence spectrum) can be regarded as a random diffusion process, spectral diffusion.

Figure 2*b* presents the path of spectral diffusion. It can be seen from this path how the fluorescence spectral shift (it was taken from Fig. 2*a*) fluctuates with time.[10] This is an example demonstrating how the environment influences a single reporter molecule. Note high resolution of the 'running commentary': at a luminescence wavelength of 592.546 nm (this corresponds to a zero in the abscissa axis in Fig. 2*a*), the molecule reports about energy changes of about 10 MHz; this corresponds to an energy resolution of $10^{-7}-10^{-8}$. A single molecule is the most sensitive sensor.

The spectral diffusion of a single terylene molecule in polyethylene at 0.03 K has been studied.[11] In this case, the excited molecule discharges the energy to high-energy phonons, which are partly used for reorganisation of the molecule environment. In turn, this reorganisation changes the orientation of the molecule, which is thus gets into a new environment. Thus, a single molecule is simultaneously a phonon generator and the detector of changes made by these phonons. Actually, we are dealing with spectral self-diffusion. The frequency of self-diffusion events (the probability of spectral jumps N) depends on the amplitude of energy jumps (Fig. 3): the greater the jump amplitude, the lower the probability. For example, a molecule experiences a 20 MHz jump 16 times, and a 40 MHz jump is made only once.

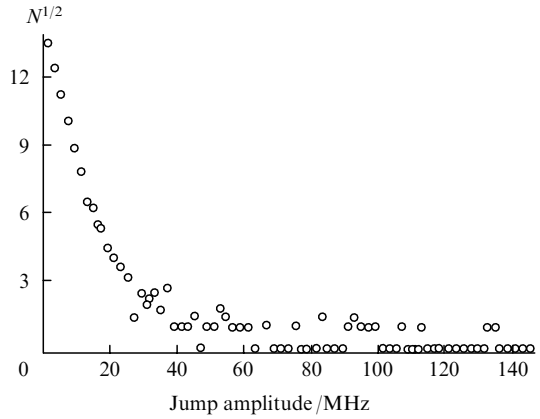


Figure 3. Probability (N) of the diffuse jumps over the spectrum as a function of the jump amplitude.[11]

The spectral self-diffusion theory provides quantitative characteristics of host–guest interactions, namely the interaction constants and spectral self-diffusion coefficients. For example, the activation energy for the phonon interaction between a single luminescent molecule of dibenzanthanthrene (DBATT)† and a naphthalene crystal has been measured.[12] It was found to be 40 cm^{-1}, which corresponds to the local vibration mode in the environment of the guest molecule.

The sensitivity of the molecular sensor is so high that it is possible to measure the external pressure applied to the crystal from the shift of luminescence lines;[13] this shift is directly proportional to the pressure, but the proportionality coefficients are different for different probe molecules. The linearity with respect to pressure describes the local compressibility of the matrix, different coefficients being indicative of the 'individuality' of the probe molecule with respect to the external pressure 'violence'.

Using molecular sensors, one can reliably measure the linear and quadratic Stark effects (line shift in an electric field) even for centrosymmetric molecules. Due to local defects in the molecular environment, the symmetry of the molecule is partially violated; as a result, an induced electric dipole equal to several millidebyes appears on the molecule;‡ even this minor dipole moment on a single molecule suffices for detecting the Stark shift.[14]

A cubic Stark effect, indicative of substantial distortion of the geometry of the DBATT molecule in the n-hexadecane crystal, has been recently observed.[15]

2. Molecular dynamics

Procedures for direct observation of the migration of single luminescent molecules based on total internal reflection microscopy have been developed. Figure 4 shows the result of this observation for a single rhodamine 6G molecule in the polyacrylamide gel.[16] Analysis of the path of the molecule may give a diffusion step, the distance distribution of the steps, the diffusion coefficient — actually, this is the visualisation of the Brownian motion of the single molecule.

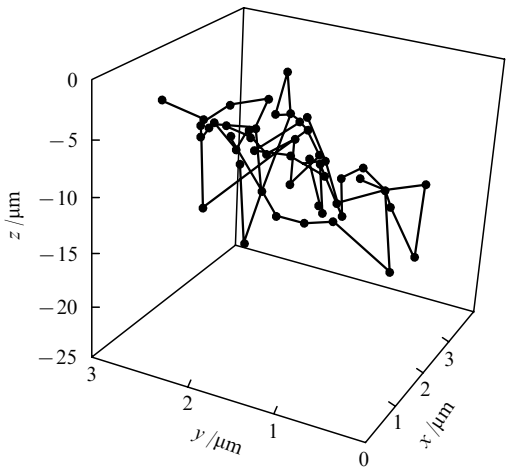


Figure 4. Three-dimensional path of the diffusion walk of a single rhodamine 6G molecule at 20 °C. The gap between the points is 0.1 s.

In some cases, this motion is unexpected and even non-Brownian (non-isotropic). For example, diffusion of rhodamine 6G in a thin polyvinylbutyral film is non-uniform: some molecules remain still, while the other move randomly and isotropically, and some other move highly anisotropically and almost unidimensionally.[17] These features can be attributed to different structures of the polymer local regions (molecular sites) in which the molecule is observed: each dictates the motion of its molecule. However, averaging of the independent paths of 97 molecules has shown[17] that the averaged motion is simultaneously Brownian and isotropic with a diffusion coefficient of 2.6×10^{-15} cm^2 s^{-1}.

Testing of the surface and surface regions at the level of single molecules is a promising line of research providing a lot of information. The dynamic probing of molecular sites is a complicated task; however the first steps have already been made. For instance, tetramethylrhodamine attached covalently through a flexible chain of atoms to a glass surface and immersed into ethylene glycol can occur in different conformation states — in some of them it moves freely, while in other it contacts with the surface. By measuring the luminescence intensity of single molecules as a function of time (in the nanosecond range and in the mode of single photon counting with time correlation analysis), it

† According to the IUPAC nomenclature, tetraceno[2,1,12,11-*opqra*]-tetracene.

‡ In glasses, due to the chaos in the arrangement of host molecules around the guest, the induced dipole on the guest molecule may be as high as 1 D.

was found that the contact of the luminophore with the surface restricts the lifetime of the excited molecule; the presence of a quencher, an azulene molecule, also shortens this time.

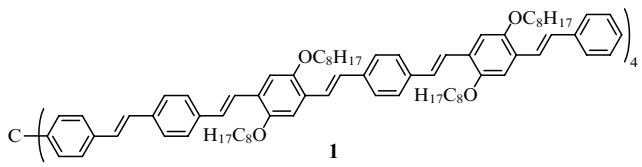
The distribution of single molecules (for arrays composed of 300 – 500 molecules) over the fluorescence times has been obtained. It was found that fluorescence times are different in the absence and in the presence of the quencher. A theory needed for the analysis of a complicated motion dynamics modulated by conformational transitions has been developed.[18]

Optical methods are especially attractive for investigating fluorescence-labelled lipids and their motion in lipid layers and on the surface of cells. The motion of molecular motors along protein threads (for example, myosin along actin) and the unidimensional motion of RNA polymerase bound non-specifically to DNA were visualised at the single molecule level. Thus the motion of tetramethylrhodamine-labelled kinesin along a protein nanotube labelled by the same luminophore at the cysteine groups has been traced. The motion takes place only in the presence of adenosine triphosphate and is physiologically 'native'. In this case, as in the case of myosin on actin, the motion of the luminescent biomolecule along the luminescent protein nanotube resembles movement of a car with switched-on headlights along a night highway with a chain of lights (if this movement is observed from above).[19]

For detecting the rotational dynamics of single molecules, luminescence is excited by polarised light; after this, emission of the polarised quanta accompanied by the loss of polarisation due to reorientation of the molecule is observed. Actually each molecule is excited many times and every time its emission is readout as an elementary event. Then the time distribution of these events is determined and the characteristic time of reorientation of the molecule is found by averaging over the events.

In solutions, reorientation times of the molecule occur in the picosecond region. By rigidly linking the luminophore to a large molecule, one can study the slow orientational dynamics of these molecules. By observing the depolarisation of the fluorescence of the fluorophore-labelled lipid molecule, the fluidity of the lipid membrane was measured.[20] This technique is of special interest for investigating the motion of the molecular-biological motors. In particular, it was shown that myosin reorientation on actin occurs jumpwise rather than as continuous rotation.[21] In some cases, motion of the fluorescent label itself is studied. The label is connected with the 'principal' molecule by a flexible bridge. This method was used to study the rotation of Texas Red attached to a DNA molecule *via* a $(CH_2)_6$ chain.[22]

If the molecule contains several freely jointed fluorescent fragments, one can study its intramolecular dynamics. As an example, consider molecule **1** in which four fluorescent fragments, namely, chains of phenylenevinylene groups, are attached to a carbon atom. Luminescence depolarisation for these four chains (arms) allows one to measure the frequency at which the molecule 'swings its arms' and to determine the resting time.[23]



1

The rotation dynamics of the rhodamine 6G molecule in supercooled *o*-terphenyl was measured based on luminescence dichroism. Rotation was detected by two sensors located at right angle to each other.[24] Each molecule was characterised by the same time of the Brownian rotation motion τ_c; however, after 10 – 100 rotation periods, the τ_c values sharply changed. These jumps of the molecule over τ_c are indicative of its motion. The characteristic time for the position change by the molecule (τ_{ex}) is on average 15 times longer than τ_c, although the temperature dependences of τ_c and τ_{ex} are the same. This means that both the rotation and the local rearrangement are motions of the same type, their temperature dependences being described by the Debye – Stokes – Einstein theory.[24]

We have already mentioned that the main function of single molecules is the reporter function. It is significant that reporter molecules (luminophores) be characterised by high quantum yields of radiation and high photostability; the latter ensures a long 'reporter' lifetime. Rhodamine 6G, Nile Red and terrylenediimine are most popular in the optics of single molecules, and green fluorescent protein GFP (see below), flavin adenine dinucleotide, *etc.* are used most widely in biology. Since recently, dendrimers have been used as luminophores.[8]

The problems of photostability of single molecules, in particular, their lifetime as a function of luminescence excitation intensity have been discussed.[25] The lifetime of the molecule and the number of photons it emits were found to sharply increase at low excitation intensities; the sensitivity of the method decreases but its information content increases.

The luminescence of single molecules has already found practical application; in particular, the single-molecule optics has been used to study the influence of the moisture content and swelling of polymers on their physicochemical properties and molecular dynamics.[26]

3. Electronic spectroscopy of single molecules

Fluorescence detection in the photon counting mode (with high time and wavelength resolutions) underlies the electronic spectroscopy of single molecules. The spectra of single molecules differ from each other in signal position (frequency shift) and width, and often also in luminescence times. This indicates that molecules occur in different environments and experience the action of different local force fields (*i.e.*, they occupy different molecular sites). As a rule, the lines in the emission spectra of single molecules are less broadened than those in usual spectra, which is indicative of the lack of non-uniform broadening caused by superposition of the spectra of various molecules; in other words, the spectrum of a single molecule rather than spectral distribution is recorded — this is a great benefit of single-molecule spectroscopy. Of particular interest is the near-field optical spectroscopy in which the emission from a molecule is collected by an optical-fibre probe.[6]

The high resolution of single-molecule spectroscopy opens up the way to direct detection of the transfer of the electron excitation energy between single donor and acceptor. The transfer efficiency is a function of the distance, the environment and the overlap of the spectra in the donor – acceptor pair; these functional dependences can be directly measured. Examples of such spectroscopic studies have been reported.[5, 8] Of particular interest is the spectroscopy of biological molecules, which provides data on the conformation, complex formation, enzyme – substrate interactions, functioning of cell elements, *etc.*

High resolution (about 10^{-4} cm^{-1}, or 10^{-8} in absolute frequency units) in the electronic spectra of single molecules can be obtained using the two-laser procedure; one laser saturates the electronic-vibrational transitions of a specified molecule, while the other (probing) one records the spectrum thus eliminating the saturation. This technique was used to detect four terylene molecules placed into a deuterionaphthalene crystal at 1.4 K.[27] The frequencies of the two lower vibration levels and the homogeneous (true) line width of the electronic-vibrational transition were measured. The measurements showed that spectra of the molecules are not identical, as the molecules occupy different positions in the host crystal.

The exciton fluorescence of a single poly(diacetylene) macromolecule in the host monomer crystal was measured at temperatures of about 6 and 60 K.[28] The macromolecule adequately simulates the semiconducting organic quantum wire. In the crystal, the fraction of the polymer chains was less than 10^{-8} and excitation was performed in the vibronic band at 501.7 nm. Both light absorption and luminescence were highly polarised

along the axis of the molecule (the linear dichroism was about 600).

A single macromolecule was represented by a single Lorentzian emission line at 2.282 eV with a half-width of 350 μeV. The line shifted somewhat to higher energies and the line width increased linearly with temperature due to the exciton–phonon interaction. The characteristic time of the loss of phase coherence by the exciton was about 2 ps. It was found that upon excitation of only one part of the macromolecule, both its parts emit, although the second part is spaced by a 10 μm distance. This means that exciton moves rather fast along the molecule by distance of $\sim$10 μm over a time period shorter than its lifetime ($\sim$110 ps). The mechanism of exciton movement has not been unambiguously established; however, irrespective of the mechanism (ballistic transport or diffusion migration), the motion velocity is high, $\sim 10^7$ cm s^{-1} for the former mechanism or 10^4 cm^2 s^{-1} for the latter.[28]

Spectroscopy of single macromolecules has been applied to study the structure and properties of conductive polymers[29] and to study functioning of the single light-storing complex LH2.[30] The complex contains 27 bacteriochlorophyll *a* molecules and 18 carotenoids. Analysis of the luminescence spectra and their dependence on polarisation of the exciting light demonstrated that excitation is concentrated on a limited number (1–3) of bacteriochlorophyll molecules.[30]

4. Quantum and non-linear optics

The key goal of quantum optics is to generate single photons 'by request'. The optical detection of single molecules in a specified mode contributes to achieving this goal. A source of photons can serve as the main unit in cryptography and communication systems and in computer systems. A highly luminescent photostable single molecule in the crystal (for example, a terylene molecule in the *p*-terphenyl crystal) may be a new candidate for this role. The possibility of using such systems in quantum optics is under active discussion.[8]

The luminescence of single molecules is closely related to the non-linear optics of single molecules, *i.e.*, non-linear interaction of the molecules with the electromagnetic field of a light wave where optical properties are functions of the light intensity. A large number of non-linear effects known for large ensembles of molecules have already been detected and studied for single molecules, for example, optical saturation, four-wave mixing, photon echo.[31]

5. Functioning of single molecules

In order to answer the question of how one molecule functions, we will consider decomposition of hydrogen peroxide induced by oxidoreductase in the presence of hydrogen donors.[32]

Horseradish peroxidase is an enzyme containing protoporphyrin IX as the key structural element. The iron ion incorporated in protoporphyrin IX participates in the redox cycle that initiates decomposition of the H_2O_2 molecule and reduction of donor molecules. Dihydrorhodamine 6G was used as the hydrogen donor; this compound does not fluoresce itself but the product of its oxidation, rhodamine 6G, is a bright luminophore.

To monitor the functioning of a single enzyme molecule, the biotinylated enzyme was immobilised on streptavidin-modified glass and placed into a buffer solution of calcium phosphate containing dihydrorhodamine 6G and H_2O_2; after that, enzyme single molecules were exposed to laser radiation. Enzyme functioning resulted in generation of rhodamine 6G, whose luminescence was detected. According to experimental conditions, free rhodamine 6G molecules quickly departed from the laser-irradiated environment of the enzyme, so that the major contribution to the luminescence was made by the molecules that had no time to leave the enzyme where they had been formed.[32]

Figure 5 shows the records of counting of the photons emitted by rhodamine 6G molecules resulting from functioning of three enzyme molecules (curves *1–3*, respectively). It can be seen that

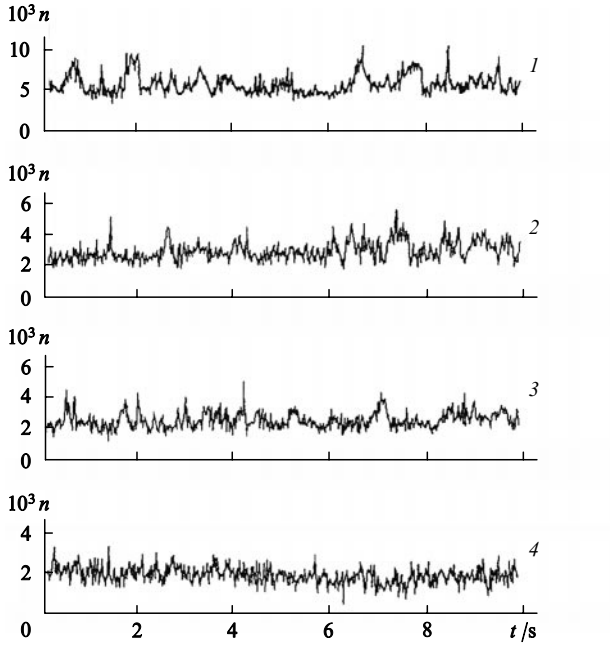


Figure 5. Number of photons *n* emitted by rhodamine 6G synthesised by three single horseradish peroxidase molecules as a function of the functioning time of these molecules (curves *1–3*). Curve *4* is the luminescence background from the region containing no enzyme molecule.[32]

over the observation period (10 s), the product yield varies, *i.e.*, periods of intensive functioning of the enzyme alternate with resting periods; moreover, the enzyme molecules 'flicker' in different ways, which is indicative of different activities of the three enzyme molecules. This difference is detected only in the case of short observation periods but disappears for longer periods. This means that the enzyme molecules behave as ergodic steady-state systems, for which time averaging is equivalent to ensemble averaging. The flickering (fluctuating) activity of the enzyme was attributed[32] (and this was convincingly proved) to different conformational states of the molecule. The conformational conversions of the enzyme change its activity and, hence, the product yield.

The energy transfer between two luminophores has been used to study the conformational dynamics of the molecule of staphylococcal nuclease, a small globular enzyme.[33] Each enzyme molecule was labelled by two luminophores: tetramethylrhodamine acting as the energy donor (it was specifically attached to the cysteine residue in the 28-position) and the cyanine dye Cy5, which was the energy acceptor (it was attached to an amino group of the protein).

Laser irradiation of single enzyme molecules induced alternating flickering luminescence of both luminophores: when one luminophore was active, the other was at rest. The flickering frequency corresponded to the frequencies of the conformational transitions in the protein that were accompanied by luminophore movement either towards or away from each other. It is noteworthy that in the presence of an inhibitor (deoxythymidine phosphate), which is bound by the nuclease active site, the conformational dynamics greatly changes. This opens up an additional source of information about the enzyme active sites.[33]

The same method was used to study the conformational behavior of α-tropomyosin in an aqueous solution.[34] This protein is a dimer composed of twisted identical chains. In both chains, luminophores were grafted on cysteine-190, in particular, Cy3-maleimide (energy donor) on one chain and Cy5-maleimide (energy acceptor) on the other chain. When two α-tropomyosin chains occurred in the twisted state, only the acceptor luminesced, while in the untwisted (denatured) state, only the donor exhibited

luminescence. The alternating flickering of the donor and acceptor luminescence observed for one α-tropomyosin molecule indicates that the two chains of this protein get twisted or untwisted at intervals. Obviously, this 'single-molecule' strategy can be used to study the association–dissociation dynamics of other biomolecules and their complexes.

The folding dynamics of the GCN4 peptide dimer has also been studied based on the label luminescence.[35] In the folded state, the peptide is a two-stranded helix. The researchers attached fluorescent labels to one ends of the strands: rhodamine 6G (energy donor) to one strand and Texas Red (energy acceptor) to the other. By the other ends (negatively charged glutamic acid residues), the dimer was immobilised, through electrostatic interaction, on the surface of glass modified by the aminopropylsiloxane groups.

In the folded dimer, both luminophores (the donor and the acceptor) are located close to each other. Therefore, on laser irradiation of the dimer and excitation of the donor, the excitation energy is transferred to the acceptor. Rhodamine 6G is thus quenched, while the Texas Red 'glows'. In the unfolded state where the donor and the acceptor are separated in space, no energy transfer from the donor to the acceptor takes place, and rhodamine 6G 'glows', while the Texas Red is quenched.

The peptide transitions from the folded to the unfolded conformation and back are detected as periodic switching-on of either donor or acceptor luminescence, which takes place in opposite phases: luminescence of one luminophore is inevitably accompanied by quenching of the other — this is clearly seen in Fig. 6. This approach is becoming popular as a general method for the study of proteins at the level of single molecules and complexes.

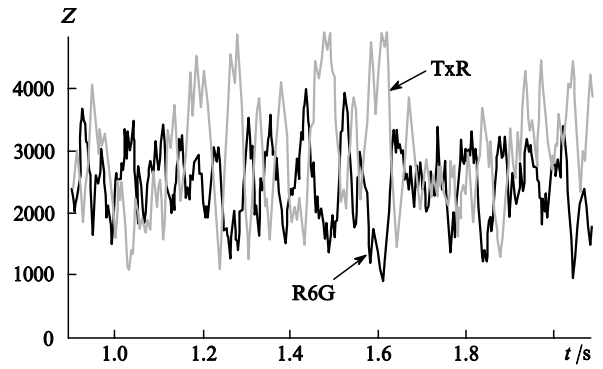


Figure 6. Luminescence, in opposite phase, of two luminophores, Texas Red (TxR) and rhodamine 6G (R6G), at functioning of a single peptide GCN4 dimer molecule.
Z is the counting rate of the emitted photons.[35]

Enzymes are not always ergodic. The two-stranded oligonucleotide, 217 bp long, labelled by tetramethylrhodamine at one end and modified by biotin at the other end, was immobilised on a streptavidin-modified glass surface due to biotin binding to streptavidin. The DNA molecule fixed in this way fluctuated between two conformational states, in one of which the label occurred near guanosine and did not luminesce (being quenched by guanosine) and in the other, the label and guanosine were separated in space; therefore, the label luminesced. The residence periods of the molecule in these two states are 0.16 and 0.03 s.[36]

Remarkably, on averaging the oscillation frequency over the time of observation of a single molecule (the lifetime of the luminophore label, which is determined by its photochemical stability), the oscillation frequencies of the light and dark periods did not depend on time, *i.e.*, each of the 37 DNA molecules studied was a time-ergodic system (this is called homogeneous ergodicity). However, the behaviour of each molecule is individual and, in this sense, the ensemble of molecules is a non-ergodic system (heterogeneous ergodicity); thus, time average is not equivalent to ensemble averaging. The reason for the non-ergodicity is the individual character of every DNA position on the glass surface. A similar heterogeneous non-ergodicity was found in a study of the catalytic activity of a single molecule of lactate dehydrogenase.[37]

Green fluorescent protein (GFP) is widely known in the molecular and cell biology;[38] it is used as a gene expression indicator and as a fluorescence label for proteins. A small (238 amino acid residues) GFP isolated from jellyfish contains, at the centre of the molecule, a strongly absorbing and luminescent chromophore, which is formed spontaneously from three amino acid residues in the presence of oxygen. The luminescence of a single GFP molecule is unique: it flickers spontaneously. The luminophore emission is excited at 488 nm and lasts for 0.4 s at low laser pumping powers. The higher the power, the shorter the emission, *i.e.*, luminescence is not only excited but also quenched by light. The dark state is stable for several minutes and returns spontaneously into the initial state capable of luminescence. Flickering is caused by the conformational transitions in the protein. The nature of flickering is still obscure; it is only known that it does not depend on the pH and is not related to GFP protonation.[8]

Single-molecule spectroscopy actively enters analytical biochemistry. The first example of the use of this method dates back to 1997.[39] The researchers obtained a chameleon protein complex consisting of the CFP and YFP proteins (CFP and YFP are mutants of the GFP with cyan and yellow fluorescence, respectively), combined by a calmodulin molecule (Ca^{2+}-binding protein).

In the absence of Ca^{2+} ions, calmodulin molecule occurs in the unfolded state; therefore, the CFP and YFP are remote from each other. Laser irradiation of CFP at a wavelength of 442 nm induces luminescence at 480 nm. After the addition of four Ca^{2+} ions, the calmodulin molecule becomes folded; as a result, the two luminophores, CFP and YFP, approach each other, and energy transfer from CFP to YFP takes place. In this case, irradiation of CFP results in YFP emission at about 530 nm. Actually, the protein complex is a highly sensitive sensor for Ca^{2+} ions: switching of the cyan fluorescence to yellow is a precise indicator for Ca^{2+} ions. Similar indicators for H^+ ions have already been developed (single-molecule pH-meter). The good prospects of this line of reseach for highly sensitive analytical and ecological chemistry are quite obvious.

An important problem in the molecular biology (in particular, neurochemistry) is the mechanism of operation of molecular motors, which ensure substance and microbody transport in the living cells. Single-molecule optics helps to answer this question. For instance, it has been used to study the movement of the protein kinesin along the microtubes composed of tubulin. Kinesin functions as a molecular motor, thus carrying various cell 'goods'. For example, it delivers the vesicle with neuromediators from the Golgi apparatus to presynaptic membranes, collects the 'containers' (*i.e.*, vesicle lipids) after liberation of neuromediators and return them to the initial 'loading' site.[8] The transport of this motor by a 8 nm distance requires hydrolysing one ATP molecule (ATP → ADP). However, neither X-ray nor electronic spectroscopy could answer the question how two ends of the kinesin molecule can extend for 8 nm.

In order to answer this question, it is necessary to study the orientational mobility of a single kinesin molecule. A kinesin mutant was prepared, in which two cysteine groups were located at a fixed distance; a reporter molecule, rhodamine, was rigidly attached to these groups (a bifunctional iodoacetamide rhodamine derivative was used for this purpose). By exciting the rigidly fixed luminescent label by polarised light and detecting luminescence polarisation of a single kinesin molecule, one can draw conclusions concerning its behaviour: whether the molecule

rotates and whether the orientation of the optical dipole changes upon kinesin functioning.

The result was unusual. It was found that polarisation of the luminescence of ADP-bound kinesin does not depend on the polarisation of the exciting light. This means that the optical dipole of a single kinesin molecule is dynamically disordered on the time scale of polarisation measurements (0.1 s), *i.e.*, the molecule (motor) executes motion averaging the optical dipole orientations. At the same time, kinesin remains bound to the microtube through both ends. This brings about the idea of a new type of motion, *viz.*, 'rolling' of kinesin along the microtube; the details of this motion are unknown as yet.[40]

Interestingly, this type of motion is characteristic only of kinesin bound to ADP, whereas ATP-bound kinesin is rigidly oriented and remains still. Thus, every ATP → ADP cycle is accompanied by movement of the 'motor' by a 8 nm distance. Undoubtedly, single-molecule optics is a brilliant tool for investigating the functioning of molecular motors.

III. Scanning tunnelling spectroscopy

The discovery of the scanning tunnelling microscopy has become a great breakthrough in the science of the nanoworld. Direct monitoring of the atomic and molecular relief of the surface has opened up the way to nanotechnology. The tip of the tunnelling microscope has become the tool for diverse operations with single atoms and molecules. The possibility of controlling tunnelling currents and atom migrations in molecules with high accuracy (0.1 Å across the surface and 0.01 Å along the height) ensures the reliability of manipulation with atoms and molecules.

Moreover, the control systems ensure a special mode of operation of the tunnelling microscope in which the tip hangs above a single atom or molecule for an arbitrarily long period.[41] This fact has immediately transformed the tunnelling microscopy into tunnelling spectroscopy of single molecules, which provided the way to their electronic-vibrational spectra and to their relaxation and chemical dynamics.

1. Visualisation of molecules and their movements

The visualisation of molecules, their 'pushing' or 'dragging' by the tunnelling tip and combination of atoms and molecules into ensembles of a specified architecture is a well-developed field of science (nanoengineering).[42] However, for chemistry, it is important to visualise chemical events (transformations and migrations of the reacting molecules and products) and monitor their evolution.

A vivid example is the discrete rotation of the O_2 molecule on the Pt(111) surface.[43] Figure 7 *a* shows the topographic view of the O_2 molecule. The 'pear-like' shape of the molecule is due to the fact that one oxygen atom 'sits' on the Pt atom; it is 'buried' and, hence, the tunnelling current from this atom is low, and it 'glows' weakly. The other atom is somewhat elevated, being located closer to the tip; the tunnelling current from this atom is greater, and the atom 'glows' more brightly.

If the tip of a tunnelling microscope is mounted above an O_2 molecule and a voltage of 0.15 V is applied to the tip, a jumpwise, counter-clockwise rotation of the molecule by 120° will take place after 20 s (Fig. 7 *b*); at the same instant, the tunnelling current will sharply diminish (Fig. 7 *d*). This indicates that the oxygen atom partly 'moves away' from under the tip. A new voltage application is accompanied by a new rotation of the molecule by 120° (Fig. 7 *c*), *etc*. This hindered oscillating rotation of the O_2 molecule between three equivalent positions on the Pt(111) surface § is induced by a low-voltage tunnelling current, the rotation velocity being proportional to the tunnelling current and the rotation

§ Three potential wells for the O_2 molecule on the Pt(111) surface shifted by 120° with respect to the centre are determined by the hexagonal symmetry of the arrangement of Pt atoms.

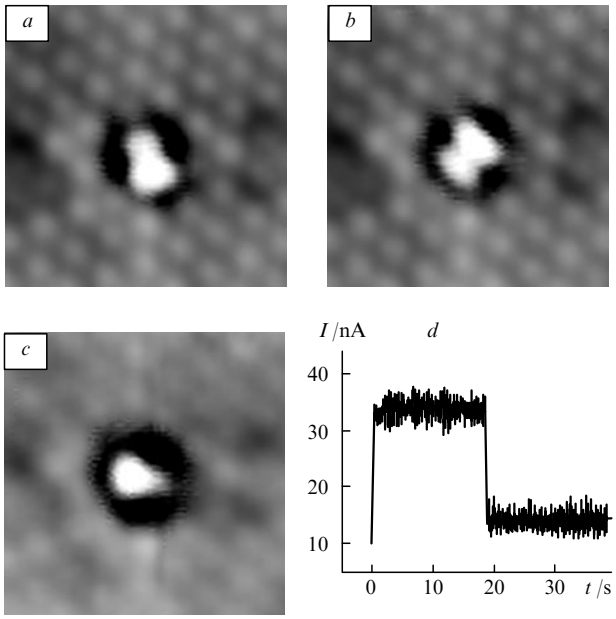


Figure 7. Topographic images of the O_2 molecule on the surface of the Pt(111) crystal during its successive angular rotations by 120° (*a*, *b*, *c*); (*d*) is the jumpwise decrease in the tunnelling current at the instant of rotation.[43]

barrier being between 0.15 and 0.175 eV (at 8 K).[43] Note that O_2 molecules not subjected to the tunnelling current remain still.

Yet another example is the rotation of an acetylene molecule on the Cu(100) surface. An acetylene molecule placed on the Cu(100) atomic surface [l(Cu – Cu) = 2.55 Å] can occupy two equivalent orthogonal positions in which the centers of the two C – H bonds fall on neighbouring Cu atoms, *i.e.*, the acetylene molecule 'lies' on two Cu atoms (Fig. 8 *a*,*b*).[44] When the tip to which the voltage is applied is located above one end of the C_2H_2 molecule (nearly above the C – H bond lying on the Cu atom), the tunnelling current jumps in a random mode between two values (Fig. 8 *c*). The jumps correspond to the instants the C_2H_2 mole-

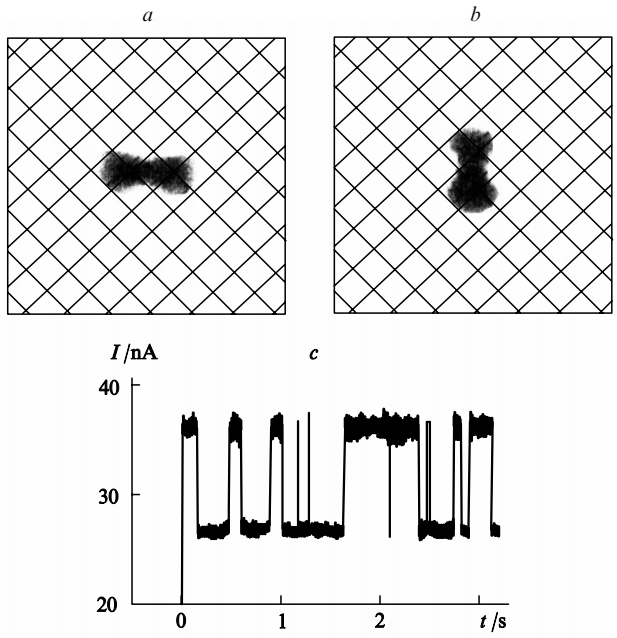


Figure 8. Topographic images of the C_2H_2 molecule in two orthogonal sites on the Cu(100) surface (*a*, *b*); (*c*) time dependence of the tunnelling current.[44]

cule hops between two orthogonal positions identical in energy. This can be clearly seen when looking at the images of the C_2H_2 molecule before and after the rotation (see Fig. 8 *a*,*b*) or from reversible fluctuations of the tunnelling current (see Fig. 8 *c*).

The rotation frequency of the acetylene molecule depends on the tip position (it is maximum when the tip is located above the C–H bond) and on the tunnelling current. The latter dependence is linear. The dependence of the rotation frequency on the voltage on the tip is not monotonic, showing a sharp maximum at the voltage where the energy of the tunnelling electrons coincides with the energy of the vibrational excitation of the C–H bond. For example, the rotation frequency of the acetylene molecule increases by an order of magnitude at a voltage of 358 mV (the frequency of C–H stretching vibrations).¶ In the case of the C_2D_2 molecule, a sharp increase in the rotation frequency (by almost two orders of magnitude) takes place at a voltage of 266 mV, which corresponds to the C–D stretching frequency.

These data indicate that the first event caused by the tunnelling current is the excitation of the C–H (or C–D for C_2D_2) bond; this is followed by the intramolecular energy transfer from the C–H stretching vibrations to bending vibrations and to vibrations of the molecule as a whole, or directly to the complex vibrations composed of the bending and rotation frequencies. The final outcome is the molecule jump from one position to the other (orthogonal). The quantitative estimates are consistent with this pattern: the probability of the orientational jump of the C_2H_2 molecule per passing (tunnelling) electron is constant and equals $\sim 10^{-10}$. Since approximately every hundredth electron excites a stretching vibration, we obtain that the probability of transformation of the stretching excitation into the rotation of the molecule as a whole is $\sim 10^{-8}$. Note that all this information — topographic images, jump frequencies, stretching vibration frequencies and the probabilities of excitation of various types of vibrations — has been gained from a single molecule.

Unlike the O_2 and C_2H_2 molecules, which rotate on the crystal surface, while remaining on the spot, an ethylene molecule migrates chaotically over the Ni(110) surface.[45] Figure 9 *a* shows that the C_2H_4 molecule jumps by arbitrary distances in an arbitrary direction in different atomic planes of the nickel single crystal, short jumps being most probable. Most of the points in Fig. 9 *a* are grouped at the centre, near the starting position of the molecule, which is designated by zero displacement. Figure 9 *b* shows the histogram of the number of jumps as a function of the jumps distance; most (almost 90%) of 112 events fall in the distance range of 0.1 – 2.0 Å.

The jumps of the ethylene molecule over the surface are in line with jumps of the tunnelling current: when the molecule moves away from under the tip, the tunnelling current sharply drops; when the molecule returns, the tunnelling current increases jumpwise to the initial value. The return of the molecule is not a rare event. Indeed, during the pulse of the tip voltage (10 s), the tunnelling current 'switches on' many times, *i.e.*, the molecule has time to move away and return back to the start hundreds of times.

The histogram of the time intervals during which the molecule is waiting for a jump from under the tip is exponential (the histograms were constructed based on observation of 300 – 1300 events with their subsequent averaging over 8 – 16 single molecules[45]). Using these histograms, the rate constants for the 'departure' of a molecule from under the tip were determined. The constants were found to depend markedly on the mass of the isotopes that form the molecle, being equal to 196, 204, 42, 24, and 15 s^{-1} for $CH_2=CH_2$, *trans*-CHD=CHD, *cis*-CHD=CHD, $CD_2=CD_2$, and $CH_2=CD_2$, respectively. It should be noted, however, that this dependence is not regular: the *trans*-CHD=CHD molecule jumps faster than *cis*-CHD=CHD and much faster than $CH_2=CD_2$ having the same mass. It has been noted[45] that for stimulation of vibrations of the molecule as a whole by the tunnelling current, it is important whether the geometric centre of the molecule (to which the tunnelling current is directed from the tip) coincides with its centre of mass. This has a crucial influence on the efficiency of pumping of the vibrational energy of the molecule by tunnelling electrons.

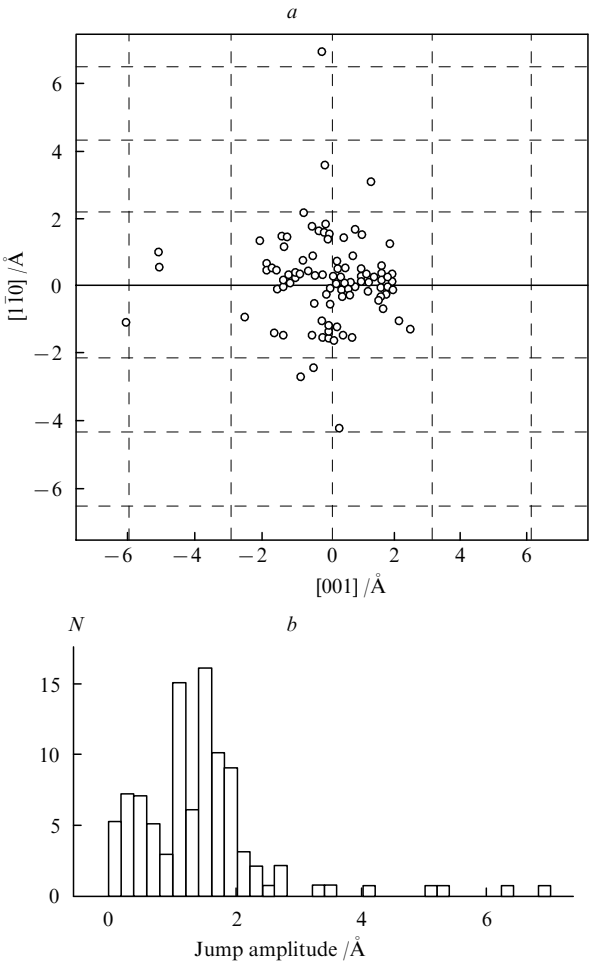


Figure 9. Distribution of the jump amplitudes of single ethylene molecules on the Ni(110) surface (*a*) and column diagram of the jumps (*b*) (*N* is the number of jumps with a given amplitude).[45]

The rate constants for the return of the ethylene molecule under the tip were measured in a similar way. For the same series of isotope-substituted ethylene molecules, they were 74, 65, 22, 21 and 6 s^{-1}. It is clear that lower constants correspond to weaker tunnelling currents. The dependence of the jump frequency on the mass of the molecule attests unambiguously to an inelastic interaction of the tunnelling electrons with the molecule, *i.e.*, to the vibrational excitation of the adsorbed molecule.

Note that the dynamic behaviour of each molecule is unique and is detected independently. There is no need to describe it by the rate constant. This value is useful only for the statistical, probabilistic characteristics of the molecule and is obtained by time averaging (over the number of migration events for one molecule) and ensemble averaging (averaging of these events over 8 – 16 individual molecules).

The migrations of the C_{60} molecule chemisorbed on silicon are also induced by the tunnelling current of about 1 nA at a voltage of 2 – 3 V.[46] It is remarkable that in this case, it is possible both to push and to pull the molecule, *i.e.*, the tip interaction with C_{60} takes place at both types of potential, namely, attraction and repulsion. The C_{60} molecule moves by steps, the step length being equal to two silicon lattice spacings. In the case where C_{60}

¶ 1 mV corresponds to 8.0655 cm^{-1}.

chemisorption implies the formation of the C–Si bond, the migration of the C_{60} molecule can be regarded as rolling conjugated with valence migration.

The conformational dynamics of individual pyrrolidine and deuterated pyrrolidine molecules on the Cu(001) surface at 9 K has been studied.[47] These molecules are attached fairly strongly to the crystal surface due to the nitrogen lone pair and occupy two positions, being arranged either at right angle to the crystal surface (position I in Fig. 10 *a*) or parallel to the surface (position II in Fig. 10 *a*). The tip mounted at a constant height above the molecule records two levels of the tunnelling current, high (0.15 nA) and low (0.03 nA) (see Fig. 10 *b*), which correspond to these two positions. The random current 'flickerings' mark precisely the reversible jumps of the molecule, while the position of the molecule on the surface remains fixed (this follows from the topographic images of the molecule).

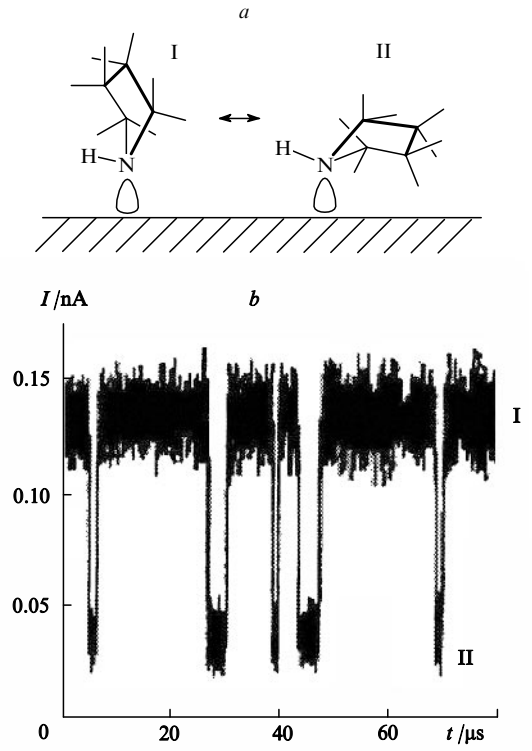


Figure 10. Arrangement of a single pyrrolidine molecule on the Cu(001) surface in two conformations I and II (*a*) and jumps of the tunnelling current upon the I ↔ II conformation transitions (*b*).[47]

By comparing the durations of two currents, one can estimate the populations of the two positions (orientations), *i.e.*, their statistical weight. Both the populations and the rate of transitions between the 'standing' and 'lying' positions (*i.e.*, the frequency of current flickering) depend on the tip voltage. It is clear that the populations are not thermodynamically equilibrated, as the molecule is exposed to the tunnelling current, which stimulates the orientational transitions.

When the transition rate is low, both orientations can be seen (see Fig. 10 *b*), while in the case of fast transitions, the tunnelling current between them is averaged. This is observed at a tip potential of 376 mV for pyrrolidine and at 283 mV for d_8-pyrrolidine. These potentials correspond to the excitation of the vibrational levels of the CH_2 and CD_2 fragments, respectively. The vibrational excitation induces fast transitions between two conformations and levelling of their populations. When the tip moves away from these resonance potentials, the slow orientation dynamics is again restored.

Two states of rigid molecules, thiophene and pyrrole, can also be clearly detected in their topographic images: in one state, molecules 'lie' on the Cu(001) surface (adsorption through the π-orbitals of the aromatic ring), while in the other one, they are arranged perpendicular to the surface ('stand'), being strongly attached to the Cu atoms by the S or N lone electron pair, respectively. Conversely, the furan molecule is weakly bound to the Cu atom; it is too labile to stay under the tunnelling current.[48] It is of interest that tetrahydrothiophene similar in structure to pyrrolidine did not show any orientational transitions under the tip current; the topographic images of tetrahydrothiophene indicate that the molecule 'stands' on the Cu atom.[48]

A special type of migration of single molecules is the controlled transfer from the surface to the tip and back; it is attained by variations of the voltage and tunnelling currents.[49] Thus the transfer of ethylene molecules is accomplished in the following way. A tungsten tip is mounted above the C_2H_4 molecule located on the Ag(110) surface. For a tunnelling current of 0.1 nA, a voltage of +70 mV is applied to the tip. While the current is maintained constant, the voltage is changed jumpwise by −70 mV and then brought gradually to −140 mV. The tunnelling current thus increases from 0.1 to 10 nA and the C_2H_4 molecule is transferred on the tip end. The back transfer takes place when the tip bearing the C_2H_4 molecule is mounted above the Ag atom and a +390 mV voltage is applied.[49] The reversible transfer of CO occurs in a similar way but at different tip potentials. Note that the physical mechanism of the transfer under these conditions is not entirely clear.

More definite considerations on the mechanism of molecular transfer were reported in another study [50] where high voltage was used to transfer the CO molecule from the Cu(111) surface to a Cu tip. When the voltage was >2 V and the distance between the tip and the surface was ~7 Å, the current was several nanoamperes. The transfer of a CO molecule to the tip mounted above this molecule or along the surface took place at a voltage exceeding the threshold value of 2.4 V. In this case, the derivative dI/dV increased. This increase coincided with the occupation of the excited $2\pi^*$-state of the CO molecule (this was determined by two-photon photoemission spectroscopy). The relaxation time of this electronically excited state was found to be very short (0.5–5.0 fs). The fast energy relaxation from the antibonding π^*-orbital of the CO molecule was the reason for the low quantum yield of carbon monoxide desorption (2.7×10^{-11} at 2.7 V or 3.0×10^{-11} at 3.0 V) and for its transfer to a new position (including the tip).

The average residence time of the CO molecule after voltage application (*i.e.*, the transfer waiting time) depended on the voltage and the current. The transfer rate (the reciprocal of the residence time) is proportional to the tunnelling current; this means that the transfer of the molecule is a single-electron process.

The isotope effect in the transfer rate has also been measured:[50] the heavy $^{13}C^{18}O$ molecules jumped to a new position under current 2.7 times more rarely than the light $^{12}C^{16}O$ molecules. The isotope effect attests to a key role of the relaxation of the electronic excitation to vibrations of the molecule as a whole. Quantitative analysis of the effect lead to an important conclusion: only 0.5% of all the tunnelling electrons excite the CO molecule to the $2\pi^*$ state and, hence, the probability of the 'jump' per excitation event is $\sim 5 \times 10^{-9}$. This is a low value but it is consistent with the low probability of electron energy relaxation to low-frequency vibrations of the molecule as a whole.

2. Tunnelling spectroscopy

The topographic images of the atomic-and-molecular surface relief are formed due to the elastic interaction of the tunnelling electrons with the surface atoms. However, probing of the energy levels of the surface atoms and molecules requires inelastic electron interaction; only inelastic interaction does involve the exchange of energy between the tunnelling electrons and surface particles. The presence of energy exchange (inelastic tunnelling)

can be detected from the current – voltage dependences the study of which constitutes the subject of tunnelling spectroscopy.

In chemistry, two versions of tunnelling spectroscopy are used most efficiently: threshold spectroscopy and resonance spectroscopy. The former was mainly developed by Ho and co-workers [51] and the latter, by Dalidchik and co-workers.[52, 53]

The threshold spectroscopy uses low potentials $V \ll \varphi$ (φ is the electron work function in the tip – surface nanocontact). The scheme of tunnelling transitions for this case is shown in Fig. 11.

The inelastic tunnelling channel opens only at a voltage exceeding the critical (threshold) value, which corresponds to the energy level of the molecule in the nanocontact. At lower voltages, the inelastic tunnelling is forbidden, as an electron cannot lose energy by sinking below the Fermi level where all electronic states are occupied and there is no room for new electrons.

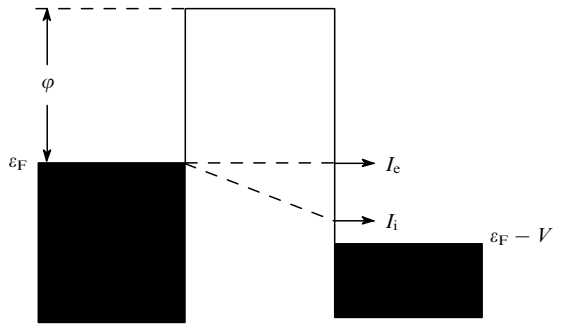


Figure 11. Scheme of tunnelling in a nanocontact at voltages $V \ll \varphi$. ε_F is the Fermi level, φ is the electron work function, I_e and I_i are elastic and inelastic tunnelling.

The threshold voltage V at which an additional inelastic tunnelling appears is recorded based on the jump in the tunnelling current $I(V)$. On excitation of the vibration frequencies of the molecule, the probability (cross-section) of the inelastic process is very low, because the probability of energy exchange between the 'light' electron and vibrations of 'heavy' atoms is low. In order to detect the vibration frequencies of single molecules based on small current $I(V)$ jumps, Ho and co-workers [51] have developed highly sensitive equipment in which they attained a high stability of the tip position above the selected molecule (the tip could stay for hours); during this period, the potential on the tip varied periodically from $-V$ to $+V$, passing a multitude (hundreds or even thousands) of times the threshold value where the jump of the tunnelling current took place. The smoothly varying and controlled voltage on the tip was modulated at a frequency of hundreds of Herz, so that the current jump was detected based on the second derivative d^2I/dV^2; the peak position in the d^2I/dV^2 *vs.* voltage V dependence corresponds to the potential V_k, which is equal to a frequency in the vibrational spectrum of the molecule.[48]

An example of such dependences for single C_2H_2 and C_2D_2 molecules on the Cu(110) surface is shown in Fig. 12. For the C_2H_2 molecule, the peak is clearly seen at 358 mV, while for C_2D_2, the peak is at 266 mV. On an energy scale, these peaks coincide with the C–H and C–D stretching frequencies, respectively. Thus, the isotope shift in the potentials corresponds to a shift in the C–H and C–D vibration frequency.[44, 51]

Threshold spectroscopy was used to obtain the spectra of diverse molecules: the $^{12}C^{16}O$ and $^{13}C^{18}O$ isotope forms,[49] ethylene and its isotope forms,[45] pyridine, benzene,[54] pyrrole, pyrrolidine, thiophene, tetrahydrothiophene and their deuterated analogues.[48] Recording of the vibrational spectrum of molecules, especially 'light ones' (for example, the spectrum of the O_2 molecule on the silver surface [49]) is far from being always possible. This is due to the fact that molecules 'run away' from under the tip earlier than a relatively reliable spectrum can be accumulated from the d^2I/dV^2 *vs.* V dependence. Possible physical reasons are

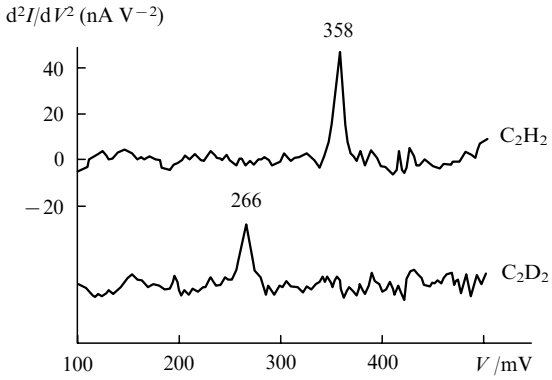


Figure 12. Second derivative of the current with respect to the voltage as a function of voltage for single C_2H_2 and C_2D_2 molecules. The voltages of 358 mV and 266 mV correspond to C–H and C–D vibration frequencies, respectively.[44]

either direct pumping, by tunnelling electrons, of the low-frequency vibrations of the molecule as a whole or the transfer of the vibrartional energy from the stretching vibrations excited by inelastically tunnelling electrons to the vibrations of the whole molecule.

The resonance tunnelling spectroscopy of single molecules developed by Dalidchik *et al.*[52, 53] operates in the field-emission mode, *i.e.*, at tip voltages exceeding the electron work function. Under these conditions, the tunnelling electrons overcome two barriers, while leaving the tip and while entering the surface (Fig. 13); therefore, they become 'captured' in the space between the tip and the molecule for about 10^{-13}–10^{-14} s. The space between the tip and the surface functions as a 'nano-scale resonator' in which stationary waves (field-emission resonances) are established at a certain value of energy. Since the energy of the resonances depends on the tip potential, the tunnelling current as a function of the voltage applied has clear-cut peaks corresponding to the electronic-vibrational (resonance) levels of the adsorbed molecule, which interacts with the electron captured by the resonator. This is a manifestation of the fundamental quantum effect, *i.e.*, the resonance clearing of the double potential barriers, which become absolutely transparent when the energy of the tunnelling electrons coincides with the vibration energies. At these resonance potentials, the tunnelling current sharply increases, thus recording the vibrational spectrum of the molecule under the tip (this is shown schematically in Fig. 13).

The resonance tunnelling spectroscopy is being actively developed by Dalidchik and co-workers since 1997.[52, 53, 55, 56] An example of the vibrational spectra of single H_2O and D_2O

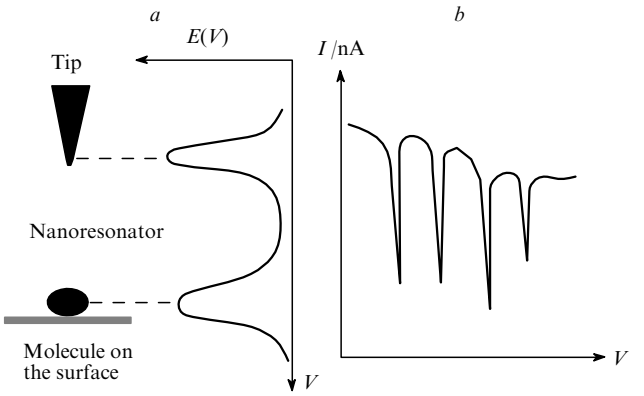


Figure 13. Scheme of a nanoresonator confined by two barriers (*a*) and schematic dependence of the tunnelling current on the voltage (*b*).

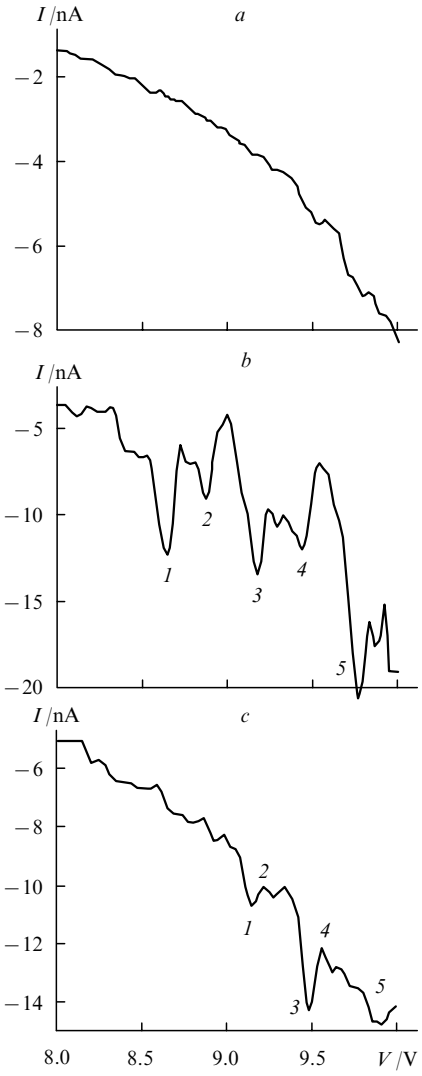


Figure 14. Tunnelling current *vs.* voltage for a clean oxidised titanium surface (*a*) and for single H_2O (*b*) and D_2O (*c*) molecules adsorbed on the oxidised titanium surface. Resonance lines (*1–5*) correspond to the vibration frequencies of the molecule (see the text).[53, 56]

molecules adsorbed on oxidised titanium is shown in Fig. 14. Here one can see the following resonance lines: $\omega_1 = e(V_3 - V_1) = 0.5$ eV and $\omega_2 = e(V_2 - V_1) = 0.2$ eV (one-quantum stretching and bending vibrations), $\omega_3 = e(V_5 - V_1) = 2\omega_1$ (two-quantum stretching vibrations) and $\omega_4 = e(V_4 - V_1) = \omega_1 + \omega_2$ (complex vibrations), where the subscripts n correspond to the numbers of resonance lines shown in Fig. 14 (V_n are the corresponding voltages).[53, 56] For the D_2O molecule, ω_1 and ω_2 are 0.35 and 0.15 eV, *i.e.*, the isotope shift corresponds almost exactly to the isotope frequency ratio $[\omega(H_2O)/\omega(D_2O) \approx \sqrt{2}]$.[56]

Figure 15 presents the vibrational spectra of molecular oxygen adsorbed on different sections of the iron oxide surface.[57] Note that the scope of resonance tunnelling spectroscopy is unlimited. This method can be used to detect and measure the frequencies of individual vibrations and their combinations; measure the vibrational relaxation rates by controlling the tunnelling current (*i.e.*, the vibrational pumping rate). The difficulties and limitations of the resonance spectroscopy are also evident: it is far from being always possible to interpret the spectrum and assign the peaks in the tunnelling current to definite vibrations; interpretation of the spectra is a difficult task, especially for polyatomic molecules. In the interpretation, it is expedient to use related molecules, isotope forms, *etc.*

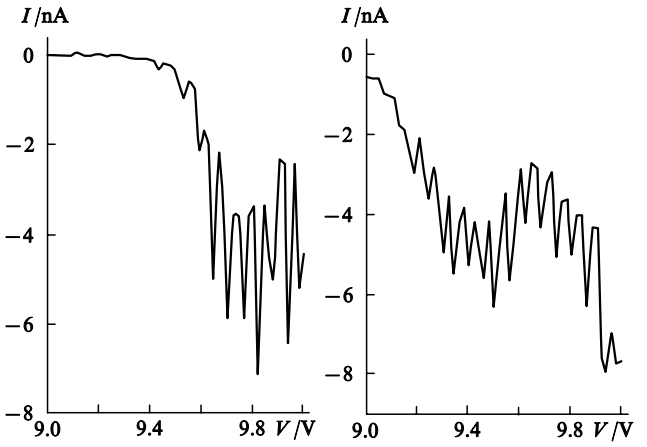


Figure 15. Vibrational spectra of oxygen molecules on different (non-identified) Fe_xO_y sites.[57]

3. The chemistry of single molecules

The inelastic interaction of the tunnelling electrons with a molecule is accompanied by pumping the molecule with vibrational energy, which stimulates its chemical transformations. These events are detected based on the images of the reactant and product, on the tunnelling current jump at the instant of reaction and on the vibrational spectra of the reactant and the products.

The simplest example is the dissociation of the O_2 molecule, physically adsorbed on the Pt(111) surface, at 40–150 K.[58] When the voltage on the tip is 0.3 V and the tunnelling current is 22 nA, dissociation of the O_2 molecule into atoms takes place in 30 s, the atoms being dispersed by three Pt(111) lattice spacings. Simultaneously, atom images and a tunnelling current jump at the instant of the reaction are observed. The rate constant for dissociation measured by statistical averaging over many molecules increases with current according to the power law I^n, where the power exponent n depends on the voltage, being equal to 0.8, 1.8 or 2.9 for voltages of 0.4, 0.3 or 0.2 V, respectively. It is of interest that the behaviour of the O_2 molecules depends on their position on the surface of a Pt crystal, in particular, they only dissociate on a *fcc* face, desorb without dissociation on the terrace steps and both dissociate and desorb on the transition bridges. It is clear that the energy pumping to the inner (reaction) vibrations competes with that to the outer vibrations of the molecule as a whole.

Yet another example is the dissociation of the C_2H_2 and C_2D_2 molecules to C_2H and C_2D on the Cu(001) surface at potentials of 2.8 and 3.9 V, respectively.[59] The resulting C_2H and C_2D species then dissociate to C_2 at potentials of 2.1 and 2.7 V, respectively. The great isotope effects are due to not only isotopy of the C–H and C–D bonds but rather by the difference in the cross-sections of excitation of the isotope molecules by tunnelling electrons. As noted above, the excitation cross-section is determined by the probability of energy transfer (inelastic process) from the 'light' electron to the 'heavy' molecule. This probability is usually very low and proportional to $(a_0/R_0)^{2\Delta v}$, where a_0 is the amplitude of the zero-point vibrations of the molecule (or atoms in it), R_0 is the equilibrium position of the oscillator simulating the vibrational subsystem, Δv is the change in the vibrational quantum number upon excitation. Thus the large isotope effect in the excitation cross-section is obvious.

The whole sequence of reactions of the single C_2H_2 and C_2D_2 molecules is reliably recorded based on images (topographic), the tunnelling current (it changes jumpwise at the instant of $C_2H_2 \rightarrow C_2H \rightarrow C_2$ transformations), vibrational spectra and isotope frequency shifts.[59]

The dehydrogenation of five isotope forms of ethylenes on the Ni(110) surface (they were considered in Section III.1) to acetylene by the tunnelling current has been studied. The process was

monitored by images and vibrational spectra of the reactant and the product. The dehydrogenation started at voltages exceeding the threshold values, the threshold voltages being different for each isotope molecule.[45] In this case, as in the case of acetylene (see above), the isotope effect is the result of competition between the energetic pumping on the internal and external vibrations of the molecule.

The single-molecule chemistry of pyridine and benzene (and their deuterated analogues) on the Cu(001) surface has been studied by spectroscopy and topography.[60] The main reaction is the dissociation of the C_5H_5N and C_6H_6 molecules to C_5H_4N and C_6H_4, respectively. For pyridine, the dissociation threshold amounts to 3.0 V; for the deuterio analogue, this is 3.2 V. The data on the molecule topography are ambiguous; only a tentative conclusion has been drawn according to which benzene 'lies' on the crystal surface, while the dissociation product, the C_6H_4 molecule, stands on the edge.[60]

The transformation of two iodobenzene molecules into biphenyl on the Cu(111) surface includes their dissociation, removal of the iodine atoms and coming together of the phenyl radicals until they are combined to form biphenyl. Each step of this process was controlled topographically and induced by the tunnelling current of the tip.[61]

Recently, Japanese researchers have published a reliable and convincing study dealing with dehydrogenation of *trans*-but-2-ene on Pd(110).[62] First, they obtained topographic images of the initial molecules (Fig. 16 *a*) and the dehydrogenation product, buta-1,3-diene (Fig. 16 *b*): the former looked like dumb-bells (the methyl groups at the ends of the molecule are elevated and provide a substantial elevation of the tip), while the latter looked like ellipses with their principal axes parallel to the row of Pd atoms. The arrangement of the *trans*-C_4H_8 and C_4H_6 molecules relative to the lattice Pd atoms is shown in Fig. 16 *c*,*d*.

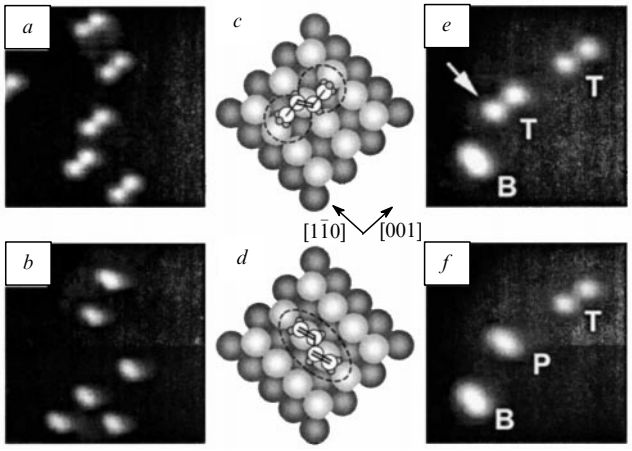


Figure 16. Topographic images of single *trans*-but-2-ene (*a*) and buta-1,3-diene (*b*) molecules, their arrangement on Pd(110) (*c*, *d*) and images of the *trans*-but-2-ene (T) molecule before the reaction (*e*) and after its transformation into buta-1,3-diene (P) (*f*). B is the initial buta-1,3-diene molecule.

Figure 16 *e* shows the initial state of the surface on which two *trans*-but-2-ene molecules (T) and one buta-1,3-diene molecule (B) are co-adsorbed. The tip of the tunnelling microscope was mounted above one of the *trans*-butene molecules (designated by the arrow in Fig. 16 *e*). At a 7 nA current and a 450 mV voltage, this molecule is converted after 1 s into the product molecule (P), which is identical to the initial buta-1,3-diene molecule (B, Fig. 16 *f*). Thus, the researchers were able to observe how *trans*-butene is dehydrogenated under the action of the tunnelling current. Probably, the hydrogen atoms are removed non-simultaneously from the methyl groups of *trans*-butene, but the intermediate structure with one removed hydrogen atom is unstable and gives off the second hydrogen atom so rapidly that its image cannot be recorded.

Spectroscopic evidence for dehydrogenation of *trans*-butene and its deuterated analogue has been derived from analysis of the $I(V)$ dependence: the second derivative d^2I/dV^2 has maxima corresponding to the C–H vibrations of the methyl group, 366 mV for *trans*-butene and 268 mV for the deuterated molecule. In the reaction product, butadiene, these frequencies are missing. Moreover, the transformation of *trans*-butene into butadiene starts at threshold voltages that exactly coincide with the frequencies of the C–H and C–D stretching vibrations.

The dependence of the reaction rate W, measured statistically for a number of molecules, on the current is a power function: $W \approx I^n$, where the power exponent n depends on the voltage and the isotope composition of the molecule and varies in the range from 1.5 to 3.0. All these features indicate unambiguously that the chemical transformation is stimulated by the vibrational excitation of the C–H (or C–D) bonds by tunnelling electrons.

A remarkable feature of the *trans*-butene molecule as an experimental object is the fact that the molecule remains motionless under the tip tunnelling current, *i.e.*, it does not move across the surface (unlike other light molecules such as O_2 or C_2H_2, considered in Sections III.1). This means that the high-frequency vibrations of the CH_3 groups interact weakly with the low-frequency vibrations of the weighty *trans*-butene molecule as a whole; therefore, the vibrational excitation of the CH_3 groups is eliminated by dissociation of the C–H (or C–D) bonds.

At the end of the discussion of studies dealing with the single-molecule chemistry, it is necessary to consider its limitations. The major one is the lack of information on the chemical transformation itself. All information on the physics of the chemical process is included in the reaction rate *vs.* current dependence ($W \approx I^n$) and in the dependence of n on V (this bears the rate of the tunnelling electrons) and on the isotope composition of the molecule. In order to extract this information, theoretical analysis of these dependences is required in terms of the theory of inelastic interaction of electrons with adsorbed molecules and energy relaxation of the molecule. This theory is well developed for gas molecules; however its extension to adsorbed molecules is an independent task. Moreover, to compare the theory with the experiment, one should know what portion of the tunnelling electrons interacts with the molecule in the inelastic mode, *i.e.*, makes a contribution to the vibrational excitation. Some estimates of this parameter for specific cases have been given above, but generally this problem is still to be solved.

IV. A single high-spin molecule as a nanomagnet

Classical nanomagnets are particles with sizes of about hundreds of nanometres. They are usually produced by dispersion or deposition of ferromagnetic materials; therefore, they are non-uniform (have particle size and magnetic moment distributions). The new class of nanomagnets, namely, single-molecule magnets, are free from these limitations. They are obtained by classical methods of chemistry and isolated and purified as pure chemical substances.[63] Like chemical 'cloning' products, single-molecule magnets are absolutely identical in size, structure and magnetism. As a rule, they are represented by high-spin metal clusters, which have a magnetic core made of transition metal atoms containing tens (or sometimes hundreds) of unpaired electrons (spin carriers) and a diamagnetic shell (coat) of organic ligands. The ligands eliminate the intermolecular exchange interaction of electrons and make the nucleus magnetically isolated (Fig. 17).

Each of these molecules is a nanomagnet, which shows all properties of a real magnet, in particular, spontaneous magnetisation, magnetisation anisotropy and hysteresis, domain structure, dynamic hysteresis (the imaginary part of the magnetisation detected based on the frequency dependence of the magnetisation in alternating fields). The exchange interaction of electrons and

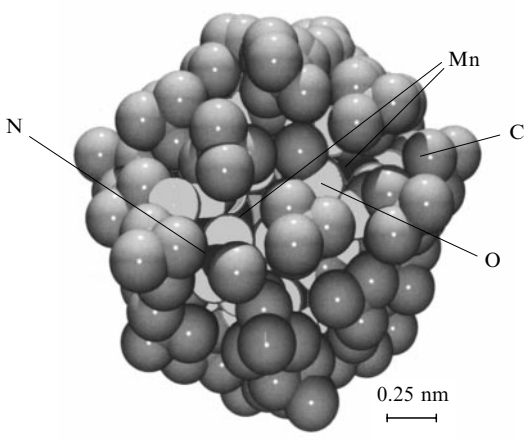


Figure 17. Three-dimensional atomic image of the molecular magnet $Mn_{30}O_{24}(OH)_8(O_2CCH_2Bu^t)_{32}(H_2O)_2(MeNO_2)_4$.[64]
All atoms except hydrogen are shown.

the dipole interaction of the electron spins within a molecule is a source of magnetism in these molecules. The exchange interactions (J) between the unpaired electrons in the core of the molecule usually have different magnitudes and signs: for some electrons they are positive and align the electron spins parallel (ferromagnetism), while for other electrons this interaction is negative and the spins become antiparallel (antiferromagnetism). As a result, the total spin of the molecule does not correspond to the number of unpaired electrons in it. For example, the number of unpaired electrons (N) in the $Mn_{12}O_{12}(O_2CMe)_{16}(H_2O)_4$ molecule is 44 while the total spin (S) is only 10 (see Ref. 63). The $Mn_9W_6(CN)_6$ and $Mn_9Mo_6(CN)_6$ molecules have the same numbers of unpaired electrons ($N = 51$) but different total spins: $S = 39/2$ and $51/2$. The total spin $S = 51/2$ implies that in the molybdenum cluster $Mn_9Mo_6(CN)_6$ all electrons are coupled ferromagnetically. In the $Fe_{11}O_6(OH)_6(O_2CPh)_{15}$ molecule, $N = 55$ and $S = 1/2$. Even for the record large molecule, $Mn_{30}O_{24}(OH)_8(O_2CCH_2Bu^t)_{32}(H_2O)_2(MeNO_2)_4$ (see Fig. 17), in which the number of unpaired electrons is 143, $S = 5$.[64]

The dipole interaction (D) of the electron spins in the $\{Mn_{30}\}$ molecule also has different signs and forms groups of spins that compose nanodomains inside the molecule. The energy of dipole interactions (normally about 1 cm^{-1}) creates a barrier to reorientation of nanodomains and is a source of dynamic and static hysteresis.

Unlike macroscopic ferromagnets, in the molecular magnets, nanodomains change the magnetisation direction by the tunnelling mechanism; therefore, a quantum hysteresis loop appears in these molecules, the discrete magnetisation steps being its typical feature (Figs 18 and 19).[63, 65]

The interest in the nanomagnet molecules is determined by the following facts:

— they are individual, identical and have a clear and exact atomic and molecular architecture;

— they are soluble and, therefore, can be easily and controllably assembled into molecular ensembles (including two-dimensional lattices on the surface);

— they have a large magnetic moment and can be reliably detected and controlled by 'point' methods, namely, atomic force and tunnelling scanning spectroscopy.

The molecular magnets attract enormous attention as elements of high-density magnetic memories and quantum computers and as materials for spintronics. About 20–30 such molecules with Mn, Fe, V, Cr, W, Tb and Dy cores have been synthesised to date.

The theory of these molecules is now under vigorous development; the conditions to be satisfied by multispin molecules for their functioning as nanomagnets have been summarised; they

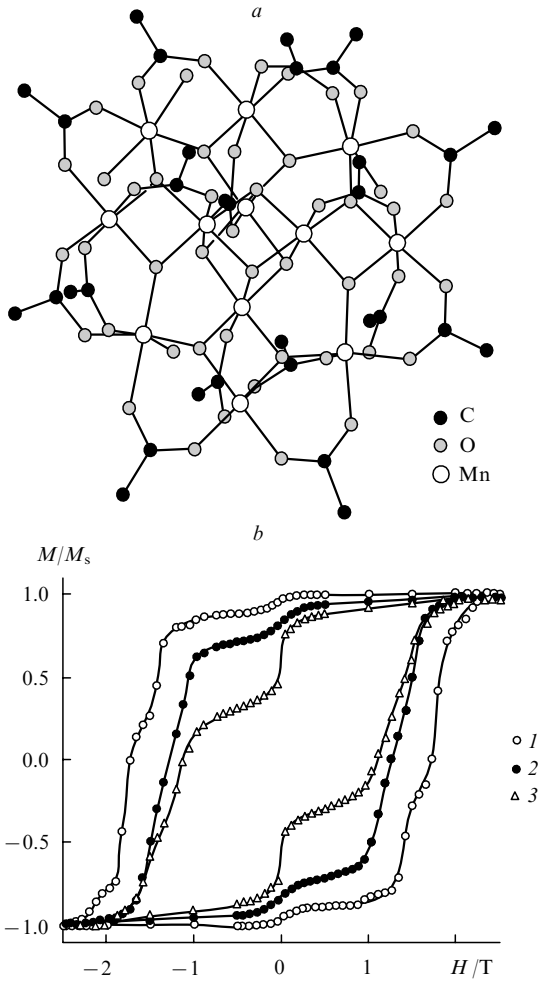


Figure 18. Atomic structure of the $Mn_{12}O_{12}(O_2CC_6H_4Cl\text{-}2)(H_2O)_4$ molecule (*a*) (the 2-chlorobenzene rings are not shown for simplicity) and quantum hysteresis loops (*b*) for the molecular nanomagnets $Mn_{12}O_{12}(O_2CMe)_{16}(H_2O)_4$ (*1*) and $Mn_{12}O_{12}(O_2CC_6H_4X\text{-}2)_{16}(H_2O)_4$ (*2*, *3*) [X = Br (*2*) and Cl (*3*)] at 20 K.[63]

include spin non-equivalence in the J and D values, the anisotropy of spin–orbit (λLS) and exchange (J) interactions. These conditions are practically implemented by combination of atoms of different metals within one molecule (in some cases, with the addition of paramagnetic organic ligands) [66] and chemical design.

In the tunnelling spectroscopy, the molecular magnets exhibit a remarkable feature, namely, spin selectivity of the inelastic interaction of the molecule with the tunnelling electrons coming out of the tip. This feature was first discovered by Dalidchik and co-workers [55] in relation to the low-spin $O_2^{-\bullet}$ molecule. The spin of the unpaired electron in the $O_2^{-\bullet}$ radical anion and the spin of the tunnelling electron create either a singlet (the total spin is equal to zero) or triplet (the total spin is equal to unity) state through the exchange interaction. These states differ energetically by the value of exchange energy; the difference results in the line splitting in the vibrational spectrum of the $O_2^{-\bullet}$ radical anions into pairs corresponding to the singlet and triplet channels of the tunnelling current (Fig. 20).

This feature opens up new opportunities for the use of molecular magnets as spin filters (for filtering the tunnelling electrons according to the spin). This is a remarkable result of the single-molecule spin chemistry, which will be undoubtedly included into the spintronics. Kozhushner and co-workers [67] proposed using a ferromagnetic tip (a source of polarised electrons) for the same purpose and developed a theory of this spin filter. An increase in the sensitivity of optical detection by micro-

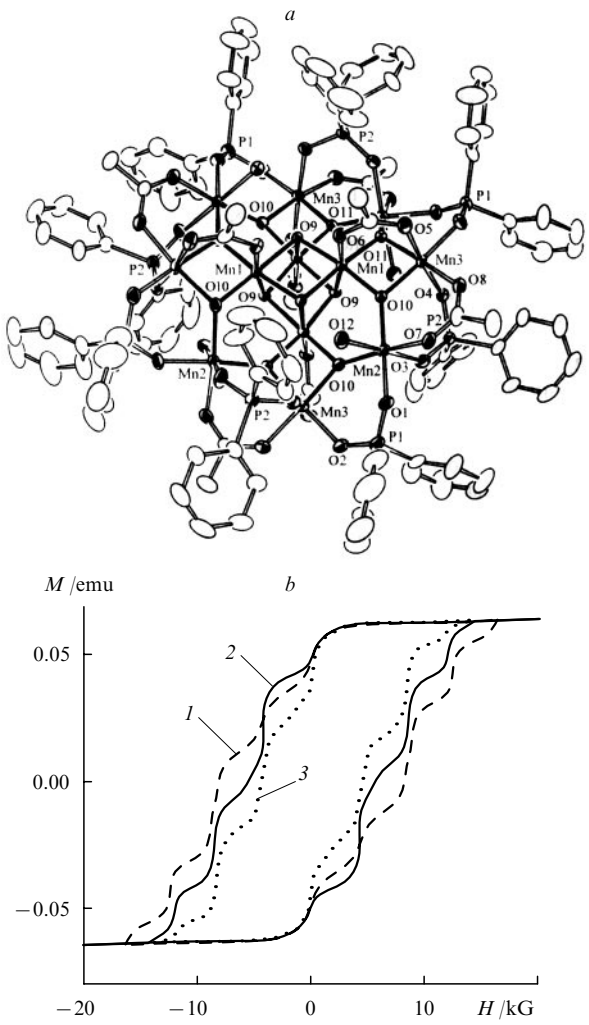


Figure 19. Atomic structure (*a*) and quantum hysteresis loops (*b*) of the molecule $Mn_{12}O_{12}(O_2CMe)_8(O_2PPh_2)_8(H_2O)_4(CH_2Cl_2)_2$ at 1.8 (*1*), 1.9 (*2*) and 2.0 K (*3*).[65]

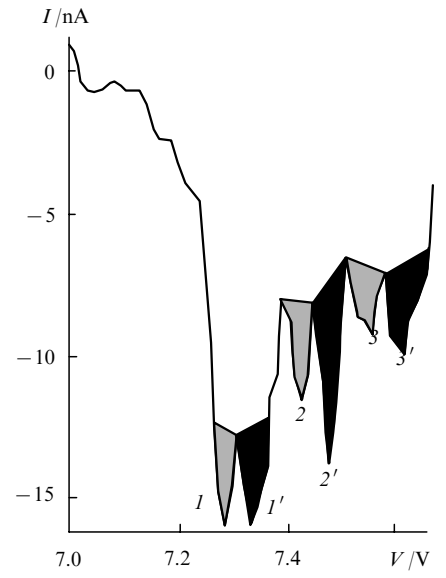


Figure 20. Tunnelling current *I vs.* potential *V* for the single $O_2^{-\bullet}$ radical anion located on the oxidised titanium surface. Line splitting within the *1*–*1′*, *2*–*2′* and *3*–*3′* pairs corresponds to the exchange energy of electrons.[56]

wave treatment of the spin molecule and the use of electron paramagnetic resonance in the tunnelling spectroscopy have been discussed.[68, 69]

V. Raman spectroscopy of single molecules

Raman spectropscopy is based on inelastic light scattering on molecular vibrations. The photons that fall on the molecule lose an energy quantum, which is spent for the excitation of molecular vibrations; this loss is detected as a shift of the exciting light frequency (Stokes shift). If the molecular vibrations have been excited, the photons falling on the molecule acquire an additional energy of molecular vibrations; as a consequence, the scattered light frequency increases (the anti-Stokes shift).

Raman spectroscopy has found wide application in the chemistry and physics of gases, liquids and solids and has become a serious supplement to the usual vibrational spectroscopy. Currently, this method is a powerful tool in the study of the molecular structure. However, the probability of inelastic photon–vibration (Raman) interaction (with generation of a Stokes or anti-Stokes line) is very low (the cross-section of this interaction does not exceed 10^{-30} cm^2 per molecule); therefore, the sensitivity of the method is low, which makes it applicable only to large ensembles of molecules.

In 1977, it was found that the probability of the inelastic light scattering by molecules sharply increases if these molecules are adsorbed on metallic surfaces,[70, 71] in particular, on metallic electrodes with an extensive surface or nanoparticles. This immobilisation results in an essential increase (10^{14}–10^{15}-, sometimes 10^{20}-fold) in the intensities of the Stokes and anti-Stokes lines, which allows one to reach the threshold of the photon–vibrational interaction cross-section, needed to detect a single molecule (about 4×10^{-18} cm^2 per molecule) and often even to exceed the threshold.[72] The best results as regards the sensitivity were obtained on adsorption of the detected molecules on Ag or Au nanoparticles with 10–100 nm size.

Two causes (two mechanisms) for the sharp increase in the probability of Raman scattering are discussed. The first one ('physical' mechanism) involves the enhancement of the local, light wave-induced electric field on the metallic surface due to the collective excitation of the conductance electrons (surface plasmon excitation). This field stimulates a strong non-linear polarisability of the molecule occurring in the vicinity of the plasmon excitation and increases sharply the probability of the photon–vibrational transition.

The second reason ('chemical' mechanism) is the specific interaction of the molecule with the metallic surface. Unlike the plasmon interaction, which is purely physical, this interaction is often called 'chemical'. The 'chemical' interaction is considered to include electron exchange between the adsorbed molecule and the surface metal atoms to yield states of the charge-transfer complex type. The electron exchange mechanism is supported by direct observations: for example, the Raman lines of the pyridine and bipyridine molecules adsorbed on silver clusters are shifted to higher frequencies, which approach those of the pyridinium cations.[71] Thus, charge transfer in the surface–adsorbed molecule system is the key element of the 'chemical' mechanism of the stimulation of Raman scattering. The reversibly generated and destroyed short-lived states are characterised by high polarisability, which is accompanied by a sharp increase in the probability of the Raman vibration transitions in the adsorbed molecule.

Both mechanisms co-exist but the contribution of each of them depends on the particular chemical systems. It is noteworthy that the predominant contribution belongs to the 'physical' mechanism. The plasmons and plasmon resonances are excited on the scale of the exciting light wavelength; this can be called a large-scale process. Conversely, the 'chemical' mechanism acts locally on a molecular scale; it refers to the local electronic interaction of the molecule with the surface.

A contribution of the 'chemical' mechanism to the enhancement of surface-induced Raman scattering has been detected.[73] Using rhodamine 6G immobilised on colloid silver clusters as an example, the researchers not only detected the contribution of the 'chemical' mechanism to the Raman scattering but also separated the contributions of the 'physical' and 'chemical' mechanisms. The solution containing colloid silver particles was placed into a chamber and a solution containing rhodamine 6G (in order to stabilise the adsorption – desorption equilibrium on the clusters) and various anions, F^-, Cl^-, Br^-, I^-, $S_2O_3^{2-}$, SO_4^{2-}, *etc*., was passed through the chamber. Measurement of the Raman scattering intensity showed that the citrate, F^- or SO_4^{2-} anions do not influence the intensity of the Raman scattering lines, Cl^-, Br^- and I^- ions enhance the Raman scattering, and the thiosulfate anions decrease scattering by 2 – 3 orders of magnitude. It was also found that the plasmon spectrum of Ag clusters does not depend on their treatment with anions. These results indicate unambiguously that both mechanisms, 'physical' and 'chemical', exist almost independently from each other, the former being universal and the other depending on the chemical pre-history of the clusters and their surface chemistry.

Rhodamine 6G is the first molecule for which the vibrational spectrum was recorded under conditions where each individual molecule was arranged above a separate silver nanocluster.[74]

The spectra of adenine and adenosine monophosphate single molecules have also been recorded on silver clusters.[75] From comparison of the Stokes and anti-Stokes line intensities for these molecules, the cross-section of the photon – vibrational interaction was calculated to be $\sim 10^{-16}$ cm^2 per molecule (this is an enormous value compared with the value of 10^{-30} cm^2, typical of the usual Raman process); it was also shown that the cross-section does not depend on the cluster size. Moreover, the spectra of both molecules were identical, *i.e*., chemical binding of adenine with the carbohydrate does not affect the Raman excitation of adenine.

For the dye Crystal Violet adsorbed on Ag and Au colloid clusters, the enhancement coefficients of the photon – vibrational interaction reach record values of 10^{20} (see Ref. 76).

The Stokes lines arise upon direct interaction of the light field with molecular vibrations; therefore, they are one-quantum. Their intensity is proportional to the intensity of the exciting light. The anti-Stokes lines result from a two-quantum process: one quantum excites a molecular vibration, while the other one induces its stimulated emission, *i.e*., takes this vibrational quantum away from the molecule. The intensity of the anti-Stokes lines is proportional to the squared intensity of the exciting light. This dependence allows one to characterise quantitatively the Raman inelastic interaction of light with molecular vibrations.

The most interesting and fruitful studies of the single-molecule Raman scattering were carried out by Sweden scientists using biologically important molecules, namely, haemoglobin[77] and horseradish peroxidase.[78] Thus comparison of the structure of Ag colloid particles bearing haemoglobin molecules, determined by scanning tunnelling spectroscopy and atomic-force microscopy, with the intensity of Raman lines of the haemoglobin molecules showed that the haemoglobin molecules confined between pairs or groups of three Ag clusters scatter the light most actively. These molecules make the major contribution to the intensities of both Stokes and anti-Stokes lines; the haemoglobin molecules fixed on dimeric clusters whose axis is parallel to the electric field vector of the exciting light being the most active. This allowed the researchers[77] to conclude (which was also confirmed by theoretical estimates) that the major contribution to the enhancement of Raman scattering on haemoglobin is made by the electric-field plasmon ('physical') mechanism but a contribution from the 'chemical' mechanism cannot be ruled out either.

Yet another biomolecule studied by this method is horseradish peroxidase immobilised on colloid silver (90 nm size).[78] In this case, the protein macromolecule becomes 'captured' by the clusters, which enhances the plasmon mechanism and increases the Raman scattering intensity. The intensity growth is so pronounced that the researchers cited[78] were able to record the Raman spectrum from a sole peroxidase molecule. Measurement of the enzymatic activity of the peroxidase demonstrated that immobilised peroxidase molecules are less active. However, if the silver clusters are pre-treated with hydrogen peroxide, the activity of the immobilised enzyme is retained at the level of the initial (non-immobilised) compound but the intensity of Raman scattering decreases.

This type of behaviour of biomolecules, in particular, enzymes, can be used as an indicator of their functioning at the single-molecule level. In some cases, it is necessary to retain also the 'native' activity of the enzyme and its high detectability by Raman spectroscopy; to this end, special techniques are used (see, for example, solution of this problem in Ref. 78).

One important fact deserves attention. To date, there is only one example where the Raman spectrum actually detects a single molecule, *viz*., peroxidase.[78] In most cases, the spectra from ensembles of single molecules are recorded, *i.e*., ensembles of isolated molecules distributed among different clusters. However, this circumstance does not depreciate in any way the chemical information and the advantages of surface-activated Raman spectroscopy.

Like the fluorescence of single molecules (see Section II), the Raman scattering ('flickering') of single molecules on the surface of metal clusters depends on time in a random manner: the spectra vary with time as regards both intensities and frequencies. This phenomenon is typical of all molecules studied including biomolecules. The random fluctuation dynamics indicates unambiguously that 'flickering' is due to the local surface – molecule interactions. The formation and decomposition of charge transfer states is accompanied by the migration of molecule across the surface. This migration changes both the intensities and frequencies of lines in the Raman spectrum of the analysed molecule.

The fluctuations are of a non-thermal nature; they are initiated by the exciting light, which generates Raman scattering. Direct experimental evidence for this statement was obtained.[79] For an ensemble of molecules (30 to 50), the frequencies (ν) and intensities (I_ν) of the Raman lines were measured and the fluctuation correlation functions were calculated

$$c(\tau) = \sum_\nu \left[\langle I_\nu(t) I_\nu(t+\tau)\rangle - \langle I_\nu(t)\rangle^2\right]$$

(the angular brackets mean averaging over τ).

The dependence $c(\tau)$ was used to obtain the fluctuation rate k. These measurements were carried out for various intensities of the light exciting the Raman spectrum. The fluctuation rate was found to increase linearly with an increase in the exciting light power. The thermal heating was minor and did not exceed 0.1 K,[79] *i.e*., the spectral fluctuations are non-thermal. This remarkable feature allows single molecules as a local dynamic surface probe.

VI. Electrical conductivity of single molecules

The particular interest in the electrical conductivity of single molecules is due to two factors. First, in chemistry (and especially in biochemistry), determination of charge conductivity of a molecule is subject to many uncertainties. For example, depending on the procedure used to determine the charge conductivity, the DNA molecule was assigned either to dielectrics, or to semiconductors, or to metallic conductors, or even to superconductors.[80] Second, a molecule as an object of molecular electronics and as an element of nanoelectronic devices (molecular resistors, diodes, single-electron transistors) requires accurate electrophysical characteristics.

The electrical conductivity of single molecules is measured using two procedures. The first one is based on a combination of atomic-force and tunnelling spectroscopy: using one of them, a single molecule is 'found', while using the other, the electrical current is applied to the molecule and measured. The second

procedure is based on direct electrochemical synthesis of the molecule (between two electrodes) and measurement of the resistance.

The first electrical conductivity measurement of a single C_{60} molecule placed between two electrodes, one being the surface of the Ag(110) crystal and the other being the tip of a tunnelling microscope, was carried out in 1995.[81] At large distances (S) from the surface of the molecule to the tunnelling tip mounted above C_{60}, the current increased exponentially with a decrease in S. When the van der Waals mechanical contact of the tip with the C_{60} molecule has been established, the current reaches a maximum value, the total resistance (R_{ef}) being 54.807 MΩ.

By substituting this R_{ef} value into the expression

$$V = R_{ef}I = R_0\left(1 + \frac{r}{t}\right)I$$

(R_0 is the electrical resistance of the C_{60} molecule, r and t are the reflection and transmission at the Fermi level†) representing Ohm's law for the molecular electrical contact, the researchers calculated the resistance (R_0) of the C_{60} molecule, which turned out to be 54.794 MΩ. After the distance from the surface of C_{60} molecule to the tip becomes smaller than the van der Waals mechanical contact, the exponential pattern of the $I(S)$ dependence is violated due to the deformation of the C_{60} molecule under the action of the tip.

The conductivity of molecules depends appreciably on their compression. For example, the compression of C_{60} by 1 Å changes the current strength that passes through the molecule by two orders of magnitude.[42] For a C_{60} molecule applied onto a dielectric, Coulomb blockade is observed at 4.2 K. The ability of the C_{60} molecule to lock the current can be used in the design of one-electron devices in which the molecule is an ideal quantum dot.[42]

The main problem in the conductivity measurement for single molecules is to create a reliable and controllable electrical contact of one molecule with two electrodes. Convenient objects are molecules containing reactive SH groups (for example, alkanedithiols); by means of these groups, molecules can be arranged as a wire between two electrodes.

An elegant and reliable experimental technique has been developed to measure the electrical conductivity of hydrocarbon $(CH_2)_n$ chains.[80] An alkanethiol monolayer with built-in alkanedithiol molecules are applied on the surface of an Au(111) single crystal from a solution. All monolayer molecules had an electrical contact with the Au surface due to S–Au covalent bonds. The upper boundary of the monolayer is formed by the terminal methyl groups of alkanethiol and (at the sites of the admixed dithiol molecules) the alkanedithiol SH groups (these groups can be single or form islets of two, three or four SH groups).

On the alkanethiol monolayer, triphenylphosphine-stabilised gold clusters were applied from a solution. The PPh_3 ligands are known to be easily exchanged with the SH groups; hence, the positions of the alkanedithiol molecules become labelled by gold clusters. Thus Au clusters are connected to the electrical contacts on the Au(111) surface through the $-S(CH_2)_nS-$ bridges. The tip of an atomic force microscope has found an Au cluster on the surface and the voltage was applied to the cluster through the $-S(CH_2)_nS-$ chain. By measuring the tunnelling current between the tip and the Au surface, the electrical conductivity of single $-S(CH_2)_nS-$ chains (Fig. 21) was found to be 0.97×10^9 Ω for $n = 8$, 2.89×10^9 Ω for $n = 9$ and 8.26×10^9 Ω for $n = 10$. From this it follows that the variation of R *vs.* n is exponential: $R \approx \exp(\beta n)$, where $\beta = 0.6$.[80]

The dependences $I(V)$ at low voltages (50 mV) proved to be linear and symmetric with respect to the sign of V. The slope of the $I-V$ straight line to the abscissa axis (axis I) corresponds to the ohmic resistance. It was found that all the R values can be divided into four groups related by the ratio 1.00 : 0.50 : 0.33 : 0.25. These values correspond to four cases of current passage, namely, through one molecule and through clusters consisting of two, three and four molecules, respectively. In the clusters, the ohmic resistance is made up from the ohmic resistances of each molecule, as in an electric circuit consisting of parallel resistors. Each molecule is an independent conductor, *i.e.*, its resistance does not depend on the neighbours in the clusters. This is a remarkable result, indicative of the reliability of the experimental technique used in the study cited.[80]

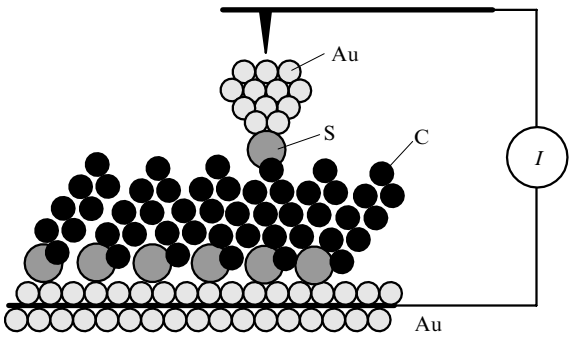


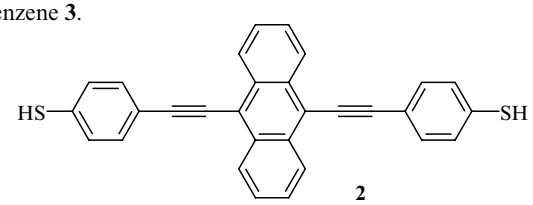
Figure 21. Scheme of the addition of electrical contacts (Au surface below and Au clusters above) to one alkanedithiol molecule incorporated in the alkanethiol monolayer.[80]

Note that the electrical resistance of the $-S(CH_2)_nS-$ chain ($R \approx 10^9$ Ω) is greater by two orders of magnitude than the resistance of the C_{60} cluster (5×10^7 Ω). It can be concluded that the conductivity of the molecule is mainly determined by the molecular orbitals, their energies and occupancies. Theoretical calculations[82] of the conductance (G) of molecular wires are consistent with this conclusion. The researchers studied the dependence of the tunnelling current in a channel (wire) on the length and on the chemical structure of molecular wires using oligo(thiophene-2,5-diylalkynediyls), oligo(phenylenealkynediyls), polyenes, *etc.*, as the wires. The conductance in the metal–wire–metal channel was calculated using the formula

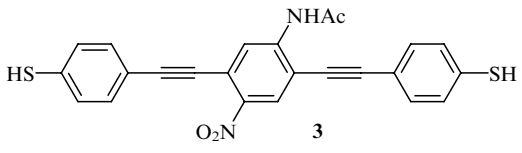
$$G = G_0\exp(-\gamma L),$$

where γ is the damping factor, L is the length of the molecular wire. The G_0 and γ values depend on the chemical structure of the molecular wire.

As another example, one can consider the measurement of the conductivity of the single molecules of 9,10-bis(*p*-mercaptophenylethynyl)anthracene (**2**) and related asymmetrically substituted benzene **3**.



2



3

For 'laying' molecules **2** and **3** between electrodes made of Au atoms, an electrode pair with one movable electrode was produced by lithography. The distance between the electrodes was 'adjusted' mechanically to the length of the molecule placed between them.

† t is the transmission coefficient corresponding to the elastic passage of the electron Bloch wave through the C_{60} molecule from one electrode to the other, r is the coefficient of reflection of this wave from the molecule.[81]

The SH groups in molecules **2** and **3** were protected by acetate groups, which were substituted by Au atoms upon incorporation of the molecules between the electrodes.[83]

The $I(V)$ plots for such molecular conductors were symmetric with respect to the sign of V. The application of a 1 V voltage to metallic surfaces gives rise to tunnelling currents of about 0.2 – 1.0 μA, which remain stable during long periods of time (up to 100 min). The electrical resistance of these molecular 'wires' was ~ 2 MΩ [almost 20 times lower than that of C_{60} and by three orders of magnitude lower than that of the aliphatic $-S(CH_2)_nS-$ chain]. It is clear that molecules **2** and **3** containing systems of highly conjugated bonds are better conductors than the C_{60} or $HS(CH_2)_nSH$ molecules; carbon nanotubes are even better conductors (their resistance is ~ 100 kΩ).

Undoubtedly, the methods for the design of molecular nanowires and nanodevices based on them will be further developed; this is a route to nanoelectronics.

VII. Mechanics and mechanochemistry of single molecules

Atomic force microscopy measures the attraction force between the microscope tip and the surface of the molecule as a function of the distance between them, unlike tunnelling scanning microscopy, which measures the current between the tip and the molecule surface. In the classical version, atomic force microscopy is contactless: the tip slides along the surface without touching it. Atomic force microscopy is also capable of visualising monoatomic vacancies on the semiconductor and dielectric surface or adsorbed molecules. This allows drawing some approximate conclusions concerning the sizes and the shapes of the molecules, their densities and arrangement on the surface. However, it should be admitted that due to the low spatial resolution, this method provides more information about the surface than about the adsorbed molecules.

The situation changes fundamentally if the atomic force microscopy is made contact, *i.e.*, one end of the molecule is attached to the tip, and the other is on the surface. Then, as the tip moves away from the surface and the molecule is being stretched, one can measure the force as a function of stretching of the molecule, *i.e.*, to study the mechanics of a single molecule. In this case, the atomic force microscopy becomes force spectroscopy.

Figure 22 shows the experimental scheme used to measure the extension (x) of a molecule and the dependence of the force (F) on drawing. The function $F(x)$ is usually non-linear (non-Hookean). The curve $F(x)$ has small local peaks, rises and dips, which are indicative of the change in the conformation of the macromolecule upon drawing. The folded conformations are replaced by extended ones under the action of drawing. Finally, at some critical elongation, the completely stretched molecule is torn; the tear strength is the strength of the chemical bond.

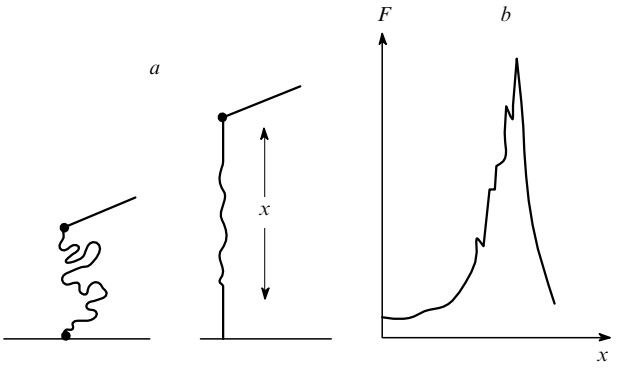


Figure 22. Scheme of the experiment with drawing of a single molecule in the atomic force microscopy (*a*) and schematic dependence $F(x)$ derived from this experiment (*b*).

Force spectroscopy has reached high sensitivity for the strength and high resolution as regards deformation and operates in a broad range of deformations and strengths: 0.01 – 100 N m^{-1} and 10^{-13} – 10^{-8} N.

The main processes in the nanomechanical technology include 'picking up' of a single molecule from a solution, a gel or a solid by the microscope tip and its drawing. During drawing, the force and deformation of the molecule are measured. This technology combines science and art: usually, the tip is immersed into a solution (or film) applied on a substrate and kept there for some period using a force of several nanonewton, and then lifted, thus drawing the molecule. By changing the functional groups at the ends of the molecule, the material of the tip and the substrate from which the molecules are taken, by varying their concentration, the amplification and the type of contact between the cantilever tip and the molecule container and using the trial-and-error method, one can attain the goal, *i.e.*, pick up the required molecule and analyse its mechanics (or mechanochemistry).

Using the new technology, it is possible to measure the binding strength of molecules and complexes (for example, DNA strands or an antigen with an antibody) and the cleavage strength of chemical bonds, to observe the conformations of molecules, to measure their elasticity and to move atoms and molecules (pull or push them over the surface).

1. Nanomechanics of macromolecules

The first outstanding success in the mechanics of single molecules was achieved in a study of natural and synthetic macromolecules. In experiments with single polysaccharide molecules, the first stage was modification of the polysaccharide terminal groups in such a way that one end could be attached to a glass surface (*via* the Si – C covalent bond) or a gold surface (Au – S bond),[84] while the other end could be grafted to the cantilever. After that, the polysaccharide molecule was drawn, while measuring the force spent for deformation. The resulting $F(x)$ dependence for these molecules was similar to that shown in Fig. 22; the Si – C bond was cleaved at a force of 2 nN, while the Au – S bond, at 1.4 nN.

The nanomechanical properties of poly(*N*-isopropylacrylamide) and poly(acrylamide) in aqueous solutions have been studied.[85] For these flexible-chain macromolecules which fold into a statistical coil, back in 1942 Kuhn derived from the freely jointed chain model the $x(F)$ dependence, which is described by the Langevin function

$$x(F) = \left[\mathrm{cth}\left(\frac{Fl}{kT}\right) - \frac{kT}{Fl}\right]L\,, \qquad (1)$$

where l is the length of the statistically independent Kuhn segment, L is the contour length of the macromolecule (the distance between the ends of the fully drawn molecule). Within the framework of this model, the Kuhn segments are considered inelastic and non-stretchable. Direct measurements of $x(F)$ for single macromolecules have shown that the function $x(F)$ is described by this model only at very low forces F (~ 10 pN), where the elasticity of the macromolecule is of purely entropic nature (the chemical bonds and angles are not strained), the elongation of the molecule being due only to the unfolding of folded conformations.

However, at $F > 10$ pN, this model does not comply with the experimental $F(x)$ dependence. If one assumes that the Kuhn segment is elastic and stretchable, the $x(F)$ dependence should be described by the generalised Langevin equation

$$x(F) = \left[\mathrm{cth}\left(\frac{Fl}{kT}\right) - \frac{kT}{Fl}\right]\left(L + \frac{nF}{K}\right), \qquad (2)$$

where n is the number of Kuhn segments ($n = L/l$), K is the elastic modulus of the Kuhn segment. The experimental data obtained

for poly(acrylamide) and poly(*N*-isopropylacrylamide) are adequately described by this function up to $F = 1000$ pN.[85]

Macromolecule	l/nm	L/nm	K/N m^{-1}
Poly(*N*-isopropylacrylamide)	0.68	460	26
Poly(acrylamide)	0.625		20

If a Kuhn segment is represented as an elastic structure, the value $K = 26$ N m^{-1} (or 26 000 dyne cm^{-1}) is indicative of a very high strength.

Note that the generalised Langevin equation (2) properly describes the elasticity of macromolecules under conditions where the intramolecular hydrogen bonds involving side groups have been destroyed (for example, in the presence of urea). However, in deionised water containing intramolecular bonds in a coil, the function $x(F)$ is no longer of the Langevin type, indicating intramolecular association.

The new atomic-force techniques have rushed like an avalanche into molecular biology.[86] Of the large number of studies, we consider below only those related to biochemistry and biophysics. Figure 23 shows the $F(x)$ dependences for single polysaccharide molecules, namely, dextran (*a*), amylose (*b*) and pullulan (*c*).[87] These dependences are described by Langevin equation (2) only at low forces and deformations.

For dextran, Eqn (2) holds for $l = 0.44$ nm (the size of a monomer unit) and $K = 14.6$ N m^{-1}. At greater deformations, the enthalpy component appears in the elasticity of the dextran molecule (a plateau on the dashed curves): the pyranose rings pass from the chair conformation to the boat conformation. The modified polymer chain is described again by the Langevin equation with the parameters $l = 0.2$ nm and $K = 34.2$ N m^{-1}, *i.e.*, the Kuhn segment becomes more elastic. In this new state, the enthalpic component of the elasticity disappears, while the entropic component is retained. The same result can be attained if the pyranose rings are destroyed by periodate oxidation: for dextran, this is attained in 180 min, for amylose, in 50 min and for pullulan, in 120 min (see Fig. 23 *a*–*c*).

Amylose and pullulan behave in a similar way. Only the entropic elasticity remains in the polymer chains formed upon destruction of pyranose rings (see Fig. 23 *d*).

The dependence $F(x)$ obtained upon drawing of the molecule of the protein titin responsible for the passive muscle elasticity is shown in Fig. 24. It can be seen from the Figure that this dependence is periodic (the curve resembles the saw teeth). The tooth period amounts to ~25 nm, while the restoring force in each tooth is 0.15–0.30 nN.[88] The periodicity is in good agreement with unfolding of the immunoglobulin titin domains. In order to verify this idea, the I8 and I4 fragments containing 8 and 4 immunoglobulin domains, respectively, were tested. The $F(x)$ curves thus obtained contained eight and four teeth, respectively, which is in full agreement with the expected result.[88] Similar dependences are also typical of another protein tenascin, a component of a territorial matrix.[89]

A serious drawback of the atomic-force spectroscopy of single molecules is ambiguity of the $F(x)$ function measured experimen-

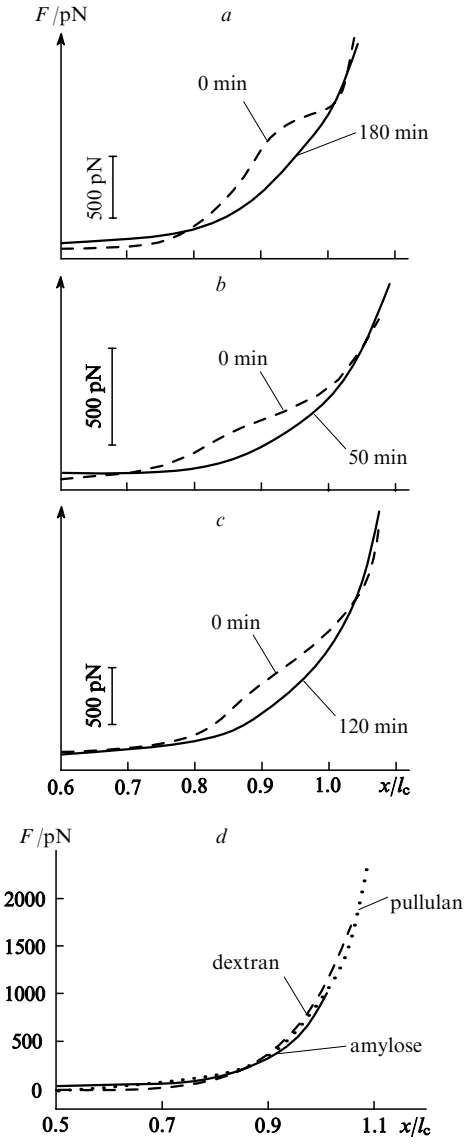


Figure 23. Force (F) *vs.* extension (x) related to the chemical bond length (l_c) for dextran [(1→6)-α-D-glycan, *a*], amylose [(1→4)-α-D-glucan, *b*) and pullulan [(1→4,1→6)-α-D-glucan, *c*] before (dashed lines) and after (continuous lines) periodate oxidation (5 mM solution of $NaIO_4$); (*d*) dependence of $F(x)$ for the same polysaccharides with the pyranose rings destroyed by periodate oxidation.[87]

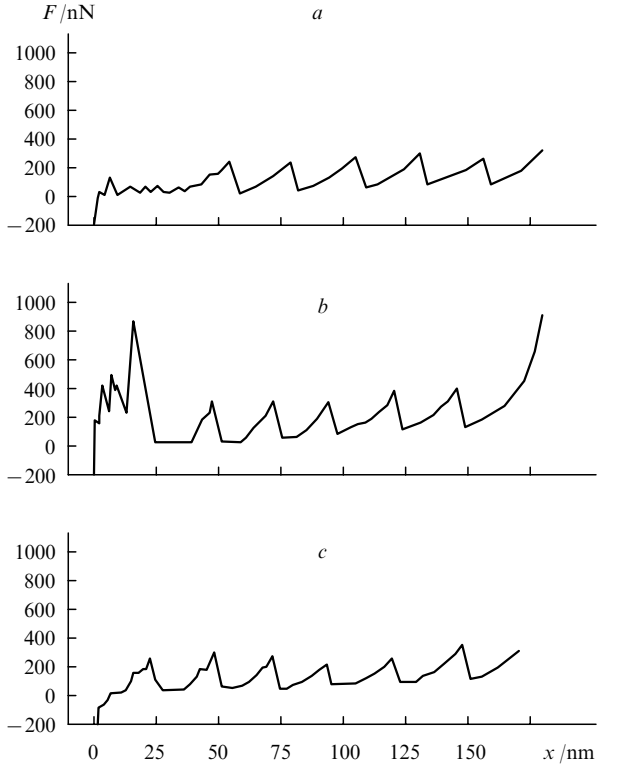


Figure 24. Force *vs.* extension of single titin molecules with various immunoglobulin domains. Domains I27–I34 (*a*), $I28_n$ (*b*), $I27_n$ (*c*).[88]

tally, which is due to the difficulty or even impracticability of determining what molecular processes and atomic rearrangements are hidden therein. Therefore, the experiment is often accompanied by molecular dynamics calculations. An example of such calculation is shown in Fig. 25. The researchers obtained the dynamic drawing curves as a function of time for one titin domain, namely, for immunoglobulin I27, with a constant force applied to it [four curves are presented, for $F = 500$ (curve *1*), 750 (*2*), 900 (*3*), and 1000 pN (*4*)]. In all cases, the initial elongation to 100 – 120 nm was followed by structure stabilisation (the molecule was not deformed for a certain period of time τ; the lower the force applied, the longer the time). However, after the period τ had elapsed, further fast deformation of the domain took place due to untangling of the protein chains.[90]

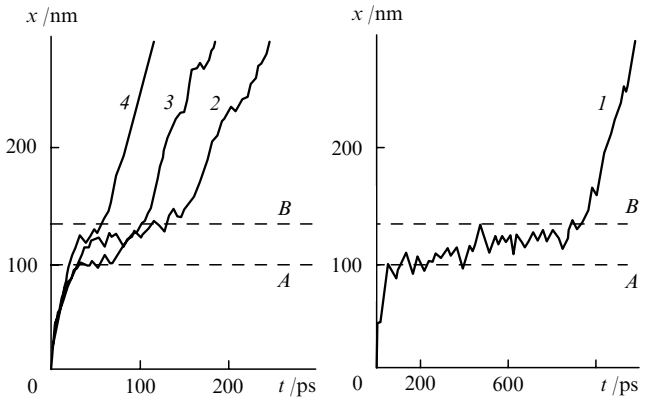


Figure 25. Dynamic (time) extensions of the domain I27 of titin at a constant force: $F = 500$ (*1*), 750 (*2*), 900 (*3*), 1000 pN (*4*). State *A* corresponds to the molecule with hydrogen bonds and state *B* corresponds to the molecule in which these bonds have been cleaved.[90]

The stable state is confined between two states *A* and *B*. In the molecule occurring in state *A*, all hydrogen bonds function and hold the chain structure; in the molecule in state *B*, six hydrogen bonds have been cleaved. A sort of plastic yielding takes place between states *A* and *B*; during this period, the molecule, while resisting deformation, sacrifices six hydrogen bonds. These results are in good agreement with experimental data and provide a clearer understanding of the molecular unfolding process (including a functioning muscle) stimulated by mechanical deformation.[90]

Considerable attention is attracted by the study of non-valence contacts in the host – guest, ligand – receptor, *etc*. systems. For a complex multipoint biotin – avidin contact, even the temperature dependence of $F(x)$ was measured. From analysis of the Poisson force distribution of the ruptures, the average strength of one contact was found to be 0.26 nN; the temperature dependence of the strength was found; in particular, as the temperature increases by 1 K, the strength decreases by 12.6 pN.[91]

Using the human serum albumin complex with a polyclonal antibody (1 : 1) as an example, the antigene – antibody interaction force was measured to be 0.244 nN.[92] The interaction of ferritin with antiferritin is described by a low adhesion force of $\sim$0.05 nN.[93] The adhesion of proteoglycans, which ensure cell recognition and aggregation, has also been studied.[94]

2. Optical tweezers and biomechanics

Recently, a new mechano-optical technology for measurement of molecule deformation has appeared. The principal working tool is an optical trap (or optical tweezer). The optical tweezer is a set of polystyrene or quartz beads of about 1 μm size. On exposure to a focussed laser beam, the bead is drawn into the focus with a force depending on the light intensity. This trap attached to the end of a molecule draws and deforms the molecule; actually, the optical trap acts as a cantilever in an atomic force microscope.

This technique is already widely used to study the structure and functioning of molecular motors.[95] ATPase, kinesin, myosin, immunoglobulin proteins — this is far from being the full list of biomolecules studied by this method.[96, 97] An impressive example is the study of operation of RNA polymerase (this enzyme accomplishes RNA transcription).[96] The researchers have fixed the RNA polymerase molecule on glass and connected it to one end of the DNA double strand, while the other end of DNA was equipped with an optical trap. It is known that RNA polymerase captures the DNA double strand and drags it through itself, while generating simultaneously the RNA thread. By exposing the optical trap to laser radiation, the researchers counterbalanced the force of DNA drawing-in by the enzyme at one end with the retention force of the DNA by the optical trap at the other end of DNA. After this balance of forces has been established, the enzyme stops operating. The balance is attained at 25 pN; this is the force at which RNA polymerase drags the DNA double helix through itself. It is believed that RNA polymerase is the most powerful known molecular motor: it is 5 – 6-fold more powerful than kinesin. Presumably, the major energy of this motor is spent for untwisting the DNA strands.

One more molecular (protein) motor, λ-exonuclease, is a component of a bacterial virus. Unlike RNA polymerase, which is energised from ATP, λ-exonuclease operates on the DNA energy: by dragging the two-stranded DNA helix through itself, it 'swallows' one of the strands. It is a weaker motor than RNA polymerase and develops only a 5 pN force.[98]

An attempt has been undertaken to use the mechano-optical technology to study topoisomerase, a remarkable enzyme, which undoes the knots on the DNA, when DNA is unpacked in a nucleus during cell division. If one understood how this enzyme operates and its operation could be terminated, it would be possible to stop the division of the malignant cells.

3. Surface nanomechanics

The controlled migration and orientation of molecules on the surface is the major route to the combination of molecules into specified ensembles, to the creation of electrical contacts, electrical circuits and integrated nanocircuits. The procedures for manipulation of single molecules on a surface rely on atomic force microscopy and tunnelling electron spectroscopy.

The force microscopy has substantially advanced in manipulating nanotubes on the surface: the microscope tip is used not only for moving nanotubes and arranging them into diverse figures and ensembles, but also for measurement of the adhesion forces between the nanotubes and the surface.[99] Various versions of this technique have been described in a review.[1] Even greater opportunities for manipulating nanoobjects are provided by tunnelling spectroscopy. In this case, the force of the tip acting on the molecule being moved is controlled by both mechanics and the electric potential of the tip. Below we present two vivid examples of operation of the nanomechanical technology.

On the (100) face of a silicon single crystal, Si_2 pairs of atoms are aligned in rows; between the rows, a gutter is formed, which accommodates the C_{60} molecules applied on the surface.[46] In the tunnelling current, the images of the C_{60} molecule look like bright domes about 2.5 nm in diameter and with a height of 0.65 nm. The potential on the tip of the tunnelling microscope, the tunnelling current and the tip elevation above the crystal surface are related in such a way that the potential and the current are maintained constant, while the distance S between the tip and the surface is variable.

The tip, which moves along the gutter, comes across the C_{60} molecule, rises and moves above the molecule (this process is described by curve *1* in Fig. 26 *a*). However, as the tip moves along the slope of C_{60}, this molecule jumps after the tip and lifts it again (this instant is shown by the arrow). These events are repeated several times, *i.e*., the C_{60} molecule jumps after the tip moving

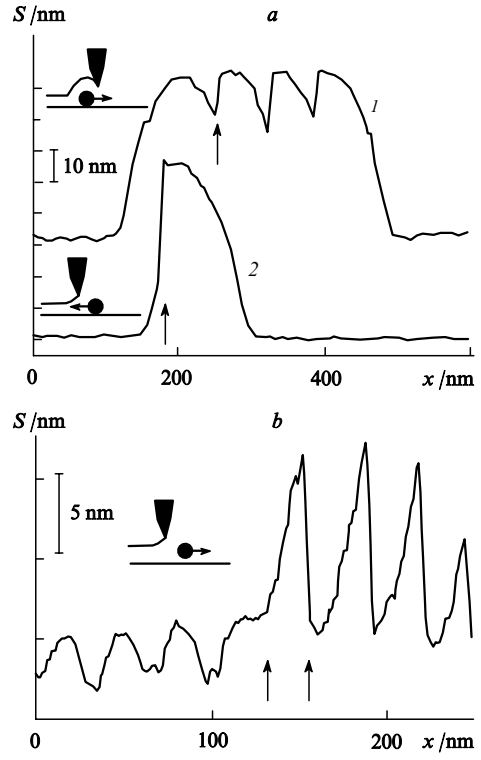


Figure 26. Vertical displacement (S) of the tip *vs.* horizontal displacement x (*a*) and horizontal displacement in the pushing mode (*b*).[46]

away. Each jump covers a discrete distance, namely, two lattice spacings of silicon. The C_{60} molecule can behave in a different way, namely, as the tip approaches the molecule, the molecule may jump towards the tip; the tip would be sharply lifted (this type of behaviour of C_{60} is described by curve *2* in Fig. 26 *a*). In both cases, the molecule and the tip interact in the attraction regime: the molecule moves either to meet or to follow the tip.

By varying the tip potential, one can also implement the repulsion regime where the moving tip pushes the molecule in front of itself. This regime is clearly illustrated in Fig. 26 *b*. In this case, the tip meets the molecule at the instant indicated by the first arrow and repels it, and the molecule jumps away by 70–80 nm (this instant is indicated by the second arrow). Then the events are repeated. Actually, the tip 'rolls' the C_{60} molecule along the gutter, each migration of the molecule being accompanied by cleavage of its chemical bond with a silicon atom and the formation of a new bond in the new position. This conclusion is based on the fact that the molecule travels every time the same distance, namely, two lattice spacings. Other distances can also be detected but their probability is much lower.[46]

Yet another example is the design of metallic monoatomic wires made of Au and Pd atoms on the NiAl(110) surface.[100] The Al atoms elevated above the (110) surface form parallel rows along the [001] direction; these rows alternate with rows of buried Ni atoms forming gutters along the same [001] direction. The Au and Pd atoms are sputtered onto the surface and then are driven together into the nickel gutters by means of a tip of a tunnelling microscope. The migration of the Au and Pd atoms starts when the distance between the atom and the tip corresponds to resistances of 150 and 50 kΩ, respectively. This means that Pd atoms are more strongly attached to the surface than the Au atoms; they migrate at tighter contacts with the tip (a smaller distance between the tip and the atom corresponds to a lower resistance).

Using this procedure, monoatomic Au and Pd nanowires and mixed wires with alternating Au and Pd atoms have been successfully obtained and their electronic properties (energy levels and densities of the electronic states, standing waves of the electron density in the atomic chains) have been studied.[100] This study opens up enormous prospects for the understanding of the electronic interactions and properties of the metal alloys through the electronic properties of 'one-dimensional' alloys, *i.e.*, metallic nanowires.

VIII. Conclusion

By the early 21st century, chemistry has reached the limit of spatial resolution. Researchers learned to detect, locate in space and recognise a single molecule and to measure almost all of its properties, to study chemical transformations and functioning of single molecules. This gave rise to a new field of chemistry: the chemistry of single molecules.

What does this new field bring to chemistry and related sciences and what findings may be expected of the further development of this discipline?

In the general chemical sense, one should hardly expect any surprises from the study of single molecules or the appearance of new, in principle, information differing from the information obtained in the studies of large ensembles of molecules.‡ Nevertheless, it is necessary to mention absolutely new information provided by single-molecule electrical conductivity measurements (for the theory of electron movement in a molecule) and by analysis of the energy fluxes in the molecule and on the surface (electronic-vibrational pumping and energy relaxation over vibrational oscillators).

One can hardly expect unusual results from the studies of functioning of single molecules. As shown by a known experiment, molecules are ergodic systems in which time averaging of the functioning of one molecule is equivalent to the ensemble averaging of instantaneous data; deviations from the ergodicity are due most often to artificial reasons (see Section II.5).

However, there is a field of chemistry for which studies of single molecules are of an inestimable value; this is the 'biological wing'. Luminescence, mechanics and mechanochemistry of single biomolecules (enzymes, proteins, nucleic acids, molecular motors, antigen–antibody type complexes, *etc.*) open almost infinite prospects in the biochemistry and biophysics.

The work with single molecules stimulates the creation of the element base for molecular electronics, nanooptics and nanomechanics. Experience in the design of high-tech devices — nanoelectronic circuits, spin filters and transistors, molecular quantum dots, nanocomputer elements, optoelectronic switches, *etc.*, is being acquired. This aspect of the chemistry and physics of single molecules is infinite. The problem of creation and functioning of logical electronic circuits on a single molecule is already discussed.[101]

The author is grateful to the Ministry of Industry, Science and Technology for financial support within the framework of the Federal Program for the Support of Leading Scientific Schools of the Russian Federation (Grant NSh 1221.2003.3) and to the Russian Academy of Sciences and the Russian Foundation for Basic Research for the support within the framework of federal programs and initiative projects.

References

1. A L Buchachenko *Usp. Khim.* **72** 419 (2003) [*Russ. Chem. Rev.* **72** 375 (2003)]
2. E J Sánchez, L Novotny, G R Holtom, X S Xie *J. Phys. Chem. A* **101** 7019 (1997)
3. H P Lu, L Xun, X S Xie *Science* **282** 1877 (1998)

‡ Certainly, it is possible to improve the quality of this information, *i.e.*, resolution and accuracy.

4. E Shera, N Seitzinger, L Davis, R Keller, S Soper *Chem. Phys. Lett.* **174** 553 (1990)
5. W P Ambrose, P M Goodwin, J H Jett, A Van Order, J H Werner, R A Keller *Chem. Rev.* **99** 2929 (1999)
6. R C Dunn *Chem. Rev.* **99** 2891 (1999)
7. P Tamarat, A Maali, B Lounis, M Orrit *J. Phys. Chem. A* **104** 1 (2000)
8. W E Moerner *J. Phys. Chem. B* **106** 910 (2002)
9. N Nilius, N Ernst, H-J Freund *Phys. Rev. B* **61** 12682 (2000)
10. W P Ambrose, W E Moerner *Nature (London)* **349** 225 (1991)
11. T Plakhotnik, E A Donley *Phys. Rev. Lett.* **87** 015504 (2001)
12. F Jelezko, B Lounis, M Orrit *J. Chem. Phys.* **107** 1692 (1997)
13. T Iwamoto, A Kurita, T Kushida *Chem. Phys. Lett.* **284** 147 (1998)
14. M Orrit, J Bernard, R I Personov *J. Phys. Chem.* **97** 10256 (1993)
15. C Brunel, P Tamarat, B Lounis, J C Woehl, M Orrit *J. Phys. Chem.* **103** 2429 (1999)
16. S Kummer, R Dickson, W E Moerner *Proc. Soc. Photo-Opt. Instrum. Eng.* **165** 3273 (1998)
17. M H Bopp, A J Meixner, G Tarrach, I Zschokke-Grinacher, L Novotny *Chem. Phys. Lett.* **263** 721 (1996)
18. M Lee, J Kim, J Tang, R M Hochstrasser *Chem. Phys. Lett.* **359** 412 (2002)
19. H Yokota, K Saito, T Yanagida *Phys. Rev. Lett.* **80** 4606 (1998)
20. G Schutz, H Schindler, T Schmidt *Opt. Lett.* **22** 651 (1997)
21. I Sase, H Miyata, S Ishiwata, K Kinosita *Proc. Natl. Acad. Sci. USA* **94** 5646 (1997)
22. T Ha, J Glass, Th Enderle, D S Chemla, S Weiss *Phys. Rev. Lett.* **80** 2093 (1998)
23. M A Summers, M R Robinson, G C Bazan, S K Buratto *Chem. Phys. Lett.* **364** 542 (2002)
24. L A Deschenes, D A Vanden Bout *J. Phys. Chem. B* **106** 11438 (2002)
25. L A Deschenes, D A Vanden Bout *Chem. Phys. Lett.* **365** 387 (2002)
26. Y Hou, D Higgins *J. Phys. Chem. B* **106** 10306 (2002)
27. T Plakhotnik, T Nonn, V Palm *Chem. Phys. Lett.* **357** 397 (2002)
28. T Guillet, J Berréhar, R Grousson, J Kovensky, C Lapersonne-Meyer, M Schott, V Voliotis *Phys. Rev. Lett.* **87** 087401 (2001)
29. D Hu, J Yu, P F Barbara *J. Am. Chem. Soc.* **121** 6936 (1999)
30. A M van Oijen, M Ketelaars, J Köhler, T J Aartsma, J Schmidt *Chem. Phys.* **247** 53 (1999)
31. P Tamarat, F Jelezko, C Brunel, A Maali, B Lounis, M Orrit *Chem. Phys.* **245** 121 (1999)
32. L Edman, Z Földes-Papp, S Wennmalm, R Rigler *Chem. Phys.* **247** 11 (1999)
33. T Ha, A Y Ting, J Liang, A A Deniz, D S Chemla, P G Schultz, S Weiss *Chem. Phys.* **247** 107 (1999)
34. Y Ishii, T Yoshida, T Funatsu, T Wazawa, T Yanagida *Chem. Phys.* **247** 163 (1999)
35. Y Jia, D S Talaga, W L Lau, H S M Lu, W E DeGrado, R M Hochstrasser *Chem. Phys.* **247** 69 (1999)
36. S Wennmalm, L Edman, R Riegler *Chem. Phys.* **247** 61 (1999)
37. Q Xue, E S Yeung *Nature (London)* **373** 681 (1995)
38. R Tsien *Annu. Rev. Biochem.* **67** 509 (1998)
39. A Miyawaki, J Llopis, R Heim, J M McCaffrey, J A Adams, M Ikura, R Y Tsien *Nature (London)* **388** 882 (1997)
40. H Sosa, E J G Peterman, W E Moerner, L S B Goldstein *Nat. Struct. Biol.* **8** 540 (2001)
41. L J Lauhon, W Ho *Rev. Sci. Instrum.* **72** 216 (2001)
42. J K Gimzewski, C Joachim *Science* **283** 1683 (1999)
43. B C Stipe, M A Rezaei, W Ho *Science* **279** 1907 (1998)
44. B C Stipe, M A Rezaei, W Ho *Phys. Rev. Lett.* **81** 1263 (1998)
45. J Gaudioso, H J Lee, W Ho *J. Am. Chem. Soc.* **121** 8479 (1999)
46. D L Keeling, M J Humphry, P Moriarty, P H Beton *Chem. Phys. Lett.* **366** 300 (2002)
47. J Gaudioso, L J Lauhon, W Ho *Phys. Rev. Lett.* **85** 1918 (2000)
48. J Gaudioso, W Ho *J. Am. Chem. Soc.* **123** 10095 (2001)
49. J R Hahn, W Ho *Phys. Rev. Lett.* **87** 166102 (2001)
50. L Bartels, G Meyer, K-H Rieder, D Velic, E Knoesel, A Hotzel, M Wolf, G Ertl *Phys. Rev. Lett.* **80** 2004 (1998)
51. B C Stipe, M A Rezaei, W Ho *Science* **280** 1732 (1998)
52. F I Dalidchik, M V Grishin, S A Kovalevskii, N N Kolchenko *Pis'ma Zh. Eksp. Teor. Fiz.* **65** 306 (1997) [a]
53. F I Dalidchik, S A Kovalevskii, B R Shub *Usp. Khim.* **70** 715 (2001) [*Russ. Chem. Rev.* **70** 627 (2001)]
54. L J Lauhon, W Ho *J. Phys. Chem. A* **104** 2563 (2000)
55. F I Dalidchik, S A Kovalevskii *Pis'ma Zh. Eksp. Teor. Fiz.* **67** 916 (1998) [a]
56. M V Grishin, F I Dalidchik, S A Kovalevskii, N N Kolchenko, B R Shub *Pis'ma Zh. Eksp. Teor. Fiz.* **66** 37 (1997) [a]
57. B R Shub, in *Problemy i Dostizheniya Fiziko-khimicheskoi i Inzhenernoi Nauki v Oblasti Nanomaterialov* (Problems and Advances of Physicochemical and Engineering Science in the Field of Nanomaterials) (Ed. V A Makhlin) (Moscow: L Ya Karpov Scientific Research Institute of Physics and Chemistry, 2002) Vols 1, 2
58. B C Stipe, M A Rezaei, W Ho, S Gao, M Persson, B I Lundqvist *Phys. Rev. Lett.* **78** 4410 (1997)
59. L J Lauhon, W Ho *Phys. Rev. Lett.* **84** 071527 (2000)
60. L J Lauhon, W Ho *Surface Sci.* **451** 219 (2000)
61. S-W Hla, L Bartels, G Meyer, K-H Rieder *Phys. Rev. Lett.* **85** 2777 (2000)
62. Y Kim, T Komeda, M Kawai *Phys. Rev. Lett.* **89** 126104 (2002)
63. D Ruiz, Z Sun, B Albela, K Folting, J Ribas, G Christou, D N Hendrickson *Angew. Chem., Int. Ed.* **37** 300 (1998)
64. M Soler, W Wernsdorfer, K Folting, M Pink, G Christou *J. Am. Chem. Soc.* **126** 2156 (2004)
65. C Boskovic, M Pink, J C Huffman, D N Hendrickson, G Christou *J. Am. Chem. Soc.* **123** 9914 (2001)
66. V S Mironov, L F Chibotaru, A Ceulemans *J. Am. Chem. Soc.* **125** 9750 (2003)
67. A L Buchachenko, M A Kozhushner, B R Shub *Izv. Akad. Nauk, Ser. Khim.* 1732 (1998) [b]
68. A L Buchachenko, F I Dalidchik, B R Shub *Chem. Phys. Lett.* **340** 103 (2001)
69. A L Buchachenko, F I Dalidchik, S A Kovalevskii, B R Shub *Usp. Khim.* **70** 611 (2001) [*Russ. Chem. Rev.* **70** 535 (2001)]
70. D Jeanmair, R Duyne *J. Electroanal. Chem.* **84** 1 (1977)
71. M G Albrecht, J A Creighton *J. Am. Chem. Soc.* **99** 5215 (1977)
72. K Kneipp, H Kneipp, I Itzkan, R R Dasari, M S Feld *Chem. Rev.* **99** 2957 (1999)
73. W Doering, S Nie *J. Phys. Chem. B* **106** 311 (2002)
74. S Nie, S R Emory *Science* **275** 1102 (1997)
75. K Kneipp, H Kneipp, V B Kartha, R Manoharan, G Deinum, I Itzkan, R R Dasari, M S Feld *Phys. Rev. E* **57** R6281 (1998)
76. K Kneipp, H Kneipp, I Itzkan, R R Dasari, M S Feld *Chem. Phys.* **247** 155 (1999)
77. H X Xu, E J Bjerneld, M Kall, L Borjesson *Phys. Rev. Lett.* **83** 4357 (1999)
78. E J Bjerneld, Z Foldes-Papp, M Kall, R Rigler *J. Phys. Chem. B* **106** 1213 (2002)
79. A Weiss, G Haran *J. Phys. Chem. B* **105** 12348 (2001)
80. X D Cui, A Primak, X Zarate, J Tomfohr, O F Sankey, A L Moore, T A Moore, D Gust, L A Nagahara, S M Lindsay *J. Phys. Chem. B* **106** 8609 (2002)
81. C Joachim, J K Gimzewski, R R Schlittler, C Chavy *Phys. Rev. Lett.* **74** 2102 (1995)
82. M Magoga, C Joachim *Phys. Rev. B* **56** 4722 (1997)
83. J Reichert, R Ochs, D Beckmann, H B Weber, M Mayor, H van Löhneysen *Phys. Rev. Lett.* **88** 176804 (2002)
84. M Grandbois, M Beyer, M Rief, H Clausen-Schaumann, H E Gaub *Science* **283** 1727 (1999)
85. W Zhang, S Zou, C Wang, X Zhang *J. Phys. Chem. B* **104** 10258 (2000)
86. H Takano, J R Kenseth, S-S Wong, J C O'Brien, M D Porter *Chem. Rev.* **99** 2845 (1999)
87. P E Marszalek, A F Oberhauser, Y-P Pang, J M Fernandez *Nature (London)* **396** 661 (1998)
88. P E Marszalek, H Lu, H Li, M Carrion-Vazquez, A F Oberhauser, K Schulten, J M Fernandez *Nature (London)* **402** 100 (1999)
89. A F Oberhauser, P E Marszalek, H P Erickson, J M Fernandez *Nature (London)* **393** 181 (1998)
90. H Lu, K Schulten *Chem. Phys.* **247** 141 (1999)
91. Y Lo, J Simons, T Beebe *J. Phys. Chem. B* **106** 9847 (2002)

92. P Hinterdorfer, W Baumgartner, H Gruber, K Schilcher, H Schindler *Proc. Natl. Acad. Sci. USA* **93** 3477 (1996)
93. S Allen, X Chen, J Davies, M C Davies, A Dawkes, J C Edwards, C J Roberts, J Sefton, S J B Tendler, P M Williams *Biochemistry* **36** 7457 (1997)
94. U Dammer, O Popescu, P Wagner, D Anselmetti, H-J Güntherodt, G Misevic *Science* **267** 1173 (1995)
95. A D Mehta, M Rief, J A Spudich, D A Smith, R M Simmons *Science* **283** 1689 (1999)
96. M D Wang, M J Schnitzer, H Yin, R Landick, J Gelles, S M Block *Science* **282** 902 (1998)
97. L Tskhovrebova, J Trinick, J A Sleep, R M Simmons *Nature (London)* **387** 308 (1997)
98. R F Service *Science* **283** 1668 (1999)
99. T Hertel, R Martel, P Avouris *J. Phys. Chem. B* **102** 910 (1998)
100. N Nilius, T Wallis, W Ho *J. Phys. Chem. B* **108** 14616 (2004)
101. S Ami, M Hliwa, C Joachim *Chem. Phys. Lett.* **367** 662 (2003)

[a] — *J. Exp. Theor. Phys. Lett. (Engl. Transl.)*
[b] — *Russ. Chem. Bull., Int. Ed. (Engl. Transl.)*